On the extreme rainfall of Typhoon Morakot (2009)

Fang-Ching Chien[1] and Hung-Chi Kuo[2]

Received 21 September 2010; revised 17 December 2010; accepted 4 January 2011; published 4 March 2011.

[1] Typhoon Morakot (2009), a devastating tropical cyclone (TC) that made landfall in Taiwan from 7 to 9 August 2009, produced the highest recorded rainfall in southern Taiwan in the past 50 years. This study examines the factors that contributed to the heavy rainfall. It is found that the amount of rainfall in Taiwan was nearly proportional to the reciprocal of TC translation speed rather than the TC intensity. Morakot's landfall on Taiwan occurred concurrently with the cyclonic phase of the intraseasonal oscillation, which enhanced the background southwesterly monsoonal flow. The extreme rainfall was caused by the very slow movement of Morakot both in the landfall and in the postlandfall periods and the continuous formation of mesoscale convection with the moisture supply from the southwesterly flow. A composite study of 19 TCs with similar track to Morakot shows that the uniquely slow translation speed of Morakot was closely related to the northwestward-extending Pacific subtropical high (PSH) and the broad low-pressure systems (associated with Typhoon Etau and Typhoon Goni) surrounding Morakot. Specifically, it was caused by the weakening steering flow at high levels that primarily resulted from the weakening PSH, an approaching short-wave trough, and the northwestward-tilting Etau. After TC landfall, the circulation of Goni merged with the southwesterly flow, resulting in a moisture conveyer belt that transported moisture-laden air toward the east-northeast. Significant mesoscale convection occurred on a long-lived east-west-oriented convergence line and on the mountain slope in southern Taiwan. This convective line was associated with large low-level moisture flux convergence caused by the northwesterly circulation of Morakot and the southwesterly flow. It is thus suggested that the long duration of Typhoon Morakot in the Taiwan area, the interaction of southwest monsoon and typhoon circulation, the mesoscale convection, and the presence of terrain are the key factors in generating the tremendous rainfall.

Citation: Chien, F.-C., and H.-C. Kuo (2011), On the extreme rainfall of Typhoon Morakot (2009), *J. Geophys. Res.*, *116*, D05104, doi:10.1029/2010JD015092.

1. Introduction

[2] Tropical cyclones (TC) are the most threatening weather system affecting Taiwan. Large numbers of typhoons form over the western North Pacific (WNP) every year, but on average, only three to four of them make landfall or have an influence on Taiwan. Strong winds and heavy precipitation associated with incoming typhoons often cause severe damage to the island. However, the major reason for the destructive power of typhoons in Taiwan is often related to the Central Mountain Range (CMR, see inset in Figure 1), a complex terrain consisting of steep mountains exceeding 3000 m. The CMR can deflect the direction of an approaching TC and significantly modify its wind and pressure patterns, resulting in enhanced precipitation and damaging winds [*Wu and Kuo*, 1999; *Wu*, 2001; *Wu et al.*, 2002].

[1]Department of Earth Sciences, National Taiwan Normal University, Taipei, Taiwan.
[2]Department of Atmospheric Sciences, National Taiwan University, Taipei, Taiwan.

0148-0227/11/2010JD015092

[3] After formation, a TC normally exhibits a motion that is closely related to advection by the surrounding environmental wind field, the steering flow, which is typically defined as the pressure-weighted average wind within an annulus (e.g., a 5–7 degree latitude radius) centered on the TC [*Chan and Gray*, 1982; *Holland*, 1984]. In fact, TC motion tends to deviate from the steering flow by a small amount. As pointed out by *Carr and Elsberry* [1990], a westward-tracking TC generally moves faster than the steering speed and shifts to the left of the steering direction in the Northern Hemisphere. Such deviation (or propagation), which is also observed in numerical simulations [*Chan and Williams*, 1987; *Fiorino and Elsberry*, 1989], is caused by the variation of the Coriolis parameter and environmental vorticity across the TC. Typhoons over the WNP typically move westward or northwestward because of the dominating steering flow controlled by the Pacific subtropical high (PSH) [e.g., *Wu et al.*, 2004]. However, in some cases when the PSH is weakening, the continental high over China is strengthening, and/or a midlatitude trough (MLT) is approaching, the TC may slow down, stall, or recurve as it approaches Taiwan. *Carr and Elsberry* [2000] showed that a TC with a westward track in the region equatorward of the

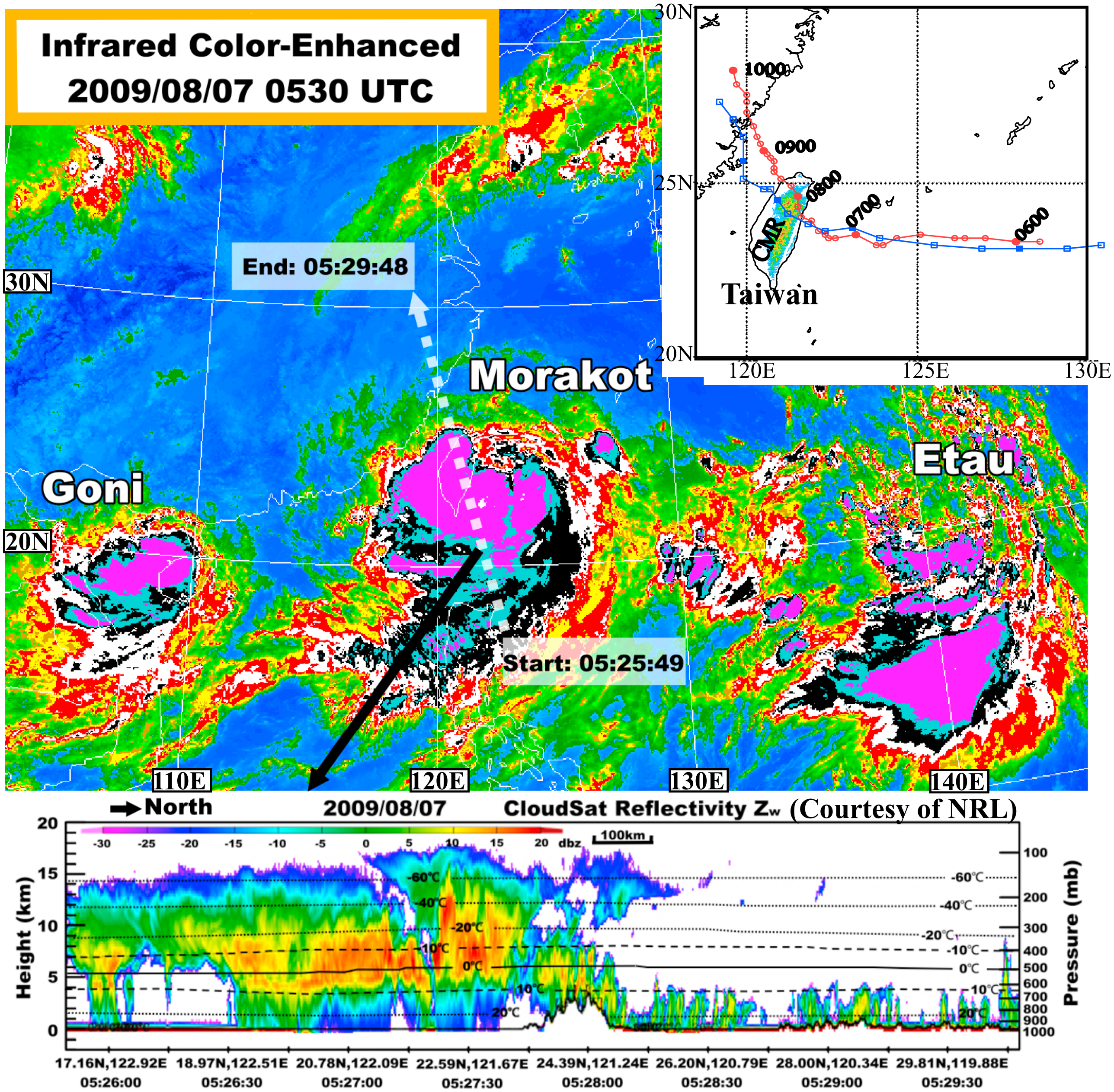

Figure 1. Infrared color-enhanced satellite images at 0530 UTC 7 August 2009. CloudSat reflectivity from 0526 UTC to 0530 UTC is shown at bottom (courtesy of Naval Research Laboratory, Monterey, California). TC tracks of Morakot are shown at top right. Blue line with squares represents the track from the JTWC best track data at a 6 h interval. Red line with dots indicates the track issued by the Central Weather Bureau of Taiwan (CWB) at a 3 h interval. Solid squares or dots with numbers (the first two digits showing date of August and the last two digits denoting the hour) denote the TC locations at 0000 UTC.

subtropical ridge axis (e.g., PSH) may turn to a more poleward heading when a developing MLT or cyclone interrupts the ridge, creating more poleward flow in the vicinity of the TC.

[4] When a TC approaches Taiwan, it can be greatly influenced and modified by the CMR. *Lin et al.* [1999] and *Wu* [2001] showed that the influence of the CMR on a westward-moving typhoon includes deceleration and southward deviation in the upstream, as well as, a quasi-stationary secondary low to the west of the CMR. There tends to be more deflection by the CMR for a weaker and slower-moving typhoon than a stronger one [*Yeh and Elsberry*, 1993a, 1993b]. Another important issue regarding typhoons crossing the CMR deals with the enhanced precipitation. *Chang et al.* [1993] used a 20 year data set from 22 surface stations to describe the effects of the Taiwan

terrain on the surface structure of typhoons. They found that the typhoon precipitation pattern in general is phase-locked with the CMR. *Wu et al.* [2002] studied Typhoon Herb (1996) with a numerical model and found that the CMR plays an important role in modifying the rainfall distribution on the island. *Lin et al.* [2002] showed that rainfall of Supertyphoon Bilis (2000) occurring in the vicinity of the topography was primarily controlled by orographic forcing rather than the TC's original rainbands. Finally, orographic rainfall can be further enhanced when typhoon circulation interacts with a superposed winter monsoonal flow [*Wu et al.*, 2009].

[5] The majority of the aforementioned papers focused primarily on the early or landfall stages of a typhoon, the former for track forecast and the latter for rainfall prediction. Not much attention, however, has been given to the late stage when TCs are moving away from Taiwan. Unfortunately, many typhoons can induce strong southwesterly flow and bring heavy precipitation over southern Taiwan when they are leaving northern Taiwan [*Chiao and Lin*, 2003]. Oftentimes, the rainfall is more intense than that brought by the typhoon itself. Strong mesoscale convective systems (MCS) can form in the warm moist southwesterly flow, which shares many common features with those of a Mei-yu front [*Trier et al.*, 1990; *Chen*, 1992; *Chen et al.*, 1998]. Typhoon Mindulle (2004), associated with strong southwesterly monsoonal flow that brought heavy rainfall and caused serious flooding and mudslides over the central and southwestern parts of Taiwan, is probably one of the best examples related to such phenomenon [*Chien et al.*, 2008; *Lee et al.*, 2008].

[6] Another good example of such events is Typhoon Morakot (2009), which brought record-breaking torrential rainfall, exceeding 3000 mm in 4 days, over southern Taiwan in August 2009. The numerous flooding and mudslides associated with the huge amount of rainfall caused tremendous loss of property and human lives. Morakot is even considered the most devastating weather event of Taiwan in the past 50 years [*Hong et al.*, 2010]. The objective of this paper is to examine the unique features of Morakot that resulted in the heavy rainfall. Specifically, the translation speed change and the southwesterly flow associated with Morakot are investigated. The paper is organized as follows. Observations of Morakot and a comparison with other landfall TCs in 1977–2009 are discussed in section 2. Using numerical data of 18 typhoons with similar track as Morakot, a composite study was performed and is presented in sections 3 and 4. Section 5 presents high-resolution analyses regarding the steering and southwesterly flow, and section 6 summarizes our major findings.

2. Observations

[7] Morakot (2009) formed over the WNP, about 1500 km east of Taiwan, at 1800 UTC 3 August 2009. It moved approximately westward toward Taiwan and then became a category-2 typhoon at 1200 UTC 5 August (inset in Figure 1). The translation speed during this period was about 20 km h^{-1} and the radii of 15 m s^{-1} and 25 m s^{-1} winds were about 250 and 100 km, respectively, as reported by the Central Weather Bureau of Taiwan (CWB). As Morakot approached Taiwan on 7 August, its translation speed slowed down to 10 km h^{-1}. The infrared (IR) satellite image at 0500 UTC 7 August (Figure 1) reveals that strong convective clouds were mostly observed in the southern quadrants of Morakot. The radar reflectivity from the National Aeronautic and Space Administration CloudSat satellite further shows that intense convection was primarily occurring to the south of the TC. This asymmetric structure implies that moisture was mainly supplied from the south, while air in the northern quadrants was relatively dry. The TC center made landfall near Hua-Lian on the east coast of Taiwan at approximately 1600 UTC 7 August, and thereafter moved very slowly toward the north-northwest. The translation speed was slower than 5 km h^{-1}. Morakot weakened and became a category-1 typhoon during its landfall because of topographic effects. About 14 h later, at 0600 UTC 8 August, the TC center crossed over the northwest coast and moved back over the ocean. Although the TC center exited Taiwan on 8 August, its circulation still greatly influenced the island until 9 August. The overall duration of Morakot, if defined by the influence period of the Taiwan area being covered within the storm radius of 15 m s^{-1} winds, was about 64 h.

[8] Due to its long duration of influence, Morakot (2009) brought record-breaking torrential rainfall over southern Taiwan, resulting in losses of about 500 million U. S. dollars and 700 fatalities. Several individual gauge stations over the mountainous regions experienced rainfall exceeding 3000 mm in the 4 day period from 6 to 9 August 2009. At these and other gauge stations, most of the rainfall actually occurred on 7 and 8 August 2009. Figure 2a shows that a 24 h accumulated rainfall exceeding 500 mm was recorded over mountainous regions of southern Taiwan on 7 August, with a maximum of approximately 800 mm. The heaviest rainfall occurred on 8 August when a large portion of southern Taiwan experienced rainfall exceeding 700 mm (Figure 2b). A number of stations even reported rainfall greater than 1200 mm.

[9] Using data from 52 typhoons that made landfall in Taiwan from 1977 to 2009, we examined the total rainfall (mm) summed over the 25 CWB surface stations, during TC landfall and during the postlandfall period (defined as the time from a TC moving back over ocean to 100 km offshore), in relation to translation speed (linear distance divided by duration time) and TC intensity (Figure 3). The intensity is defined by TC maximum wind speed right before TC landfall from CWB's official report. Comparing Figure 3a with Figure 3b, we notice that the total rainfall often was larger during the landfall period than during the postlandfall period. However, similar to several other TCs including Typhoons Sinlaku (2008) and Haitang (2005), Morakot produced more precipitation in the postlandfall period than in the landfall period (see also Figure 2). Figure 3 also suggests that the amount of rainfall in Taiwan was in general related to the TC translation speed (the slower the speed, the larger the rainfall), but not the TC intensity. In addition, Figure 3 indicates that there were more heavy rain events in the second half of the era (i.e., 1994 to 2009) than the first half. It may be related, in part, to more typhoons approaching the Taiwan area (as opposed to the case that fewer typhoons approached the SCS in the last 10–20 years) as a result of decadal TC track changes [e.g., *Liu and Chan*,

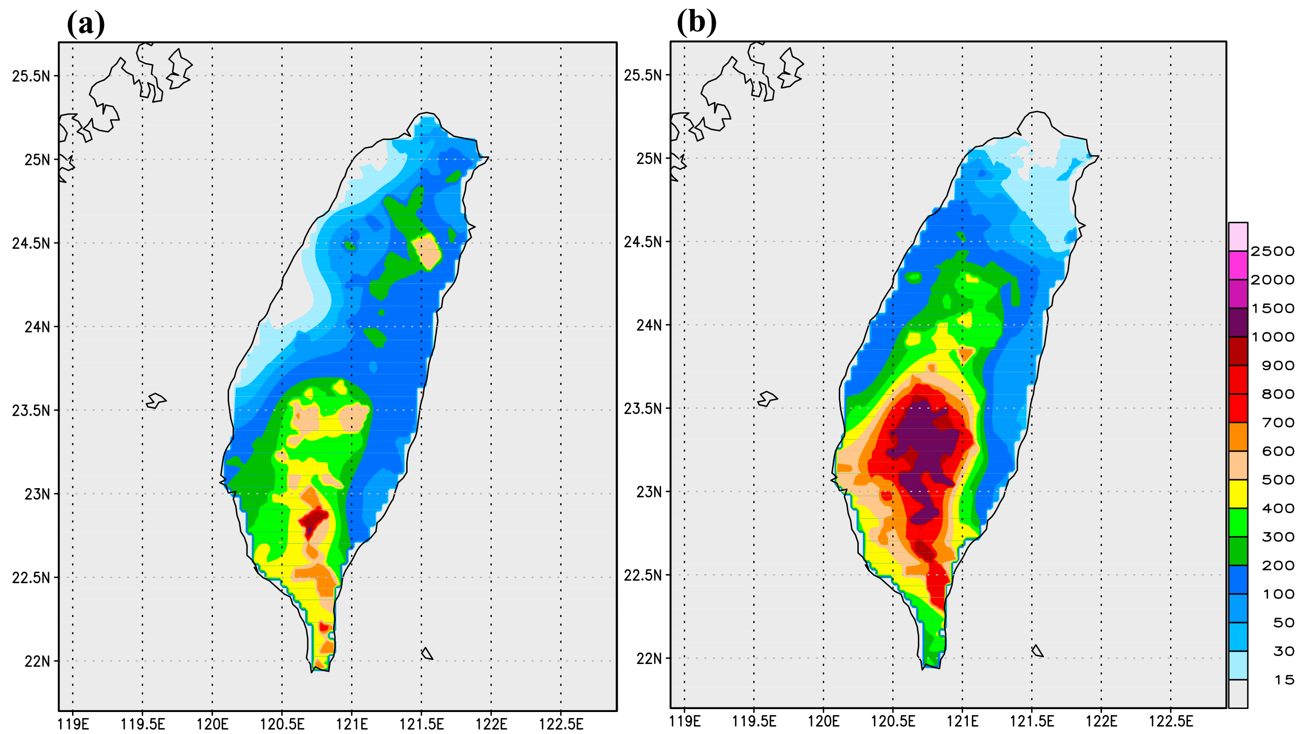

Figure 2. The 24 h observed rainfall (mm) accumulated (a) from 0000 UTC 7 August to 0000 UTC 8 August and (b) from 0000 UTC 8 August to 0000 UTC 9 August 2009.

2008]. In any event, the tendency of increasing rainfall intensity in more recent decades is certainly a major concern to the society and deserves more attention in future studies.

[10] Figure 4 further shows the total rainfall as a function of the reciprocal of TC translation speed (s m^{-1}), along with the lines of regression and standard deviation. (The reason that we chose this speed rather than the normal speed as the abscissa is because the regression shows that rainfall is nearly proportional to the reciprocal of translation speed. In addition, the plot could easily highlight those slower TCs by placing them to the right side of Figure 4.) Figure 4a clearly indicates that during TC landfall, rainfall was nearly proportional to the reciprocal of TC translation speed, rather than TC intensity. In other words, the slower a TC passes Taiwan (the longer duration time), the more rainfall it can bring to the island. Morakot was slower than most storms and thus produced more precipitation. The coefficient of determination (R^2) in the regression is 0.54 and only Typhoon Nari (2001) is outside the range of 1 standard deviation. What makes Morakot a remarkable storm happened in the postlandfall period during which the total rainfall over the island increased and became exceptionally large, compared with other TCs (Figure 4b). This positioned Morakot far outside the range of one standard deviation, implying that additional explanations other than the slow translation speed are required. We will show that strong southwesterly flow played an important role in supplying the moisture and producing long-lived mesoscale convection for the rainfall of this period, which also happened in Sinlaku (2008) and Mindulle (2004).

[11] During Morakot's landfall, clouds over southwestern Taiwan were not particularly deep, but they were associated with very intense convection shown in the radar reflectivity at 0000 UTC 8 August (Figure 5a). The convection developed along an east-west-oriented line because it was caused by strong low-level convergence between the northwesterly flow of the TC circulation and the southwesterly flow. This is similar to the Mindulle case as presented by *Chien et al.* [2008]. The convective line was nearly stationary for around 10 h before slowly moving northward at 1200 UTC 8 August (Figure 5b). Many MCSs embedded in the convective line developed and dissipated one after another, supporting the long-lived convective line (~33 h). When over land, the MCSs were further enhanced by the high terrain in southern Taiwan, resulting in torrential rainfall over the mountainous regions. By 0000 UTC 9 August (Figure 5c), the convective line had moved only about 50 km northward during the past 24 h. This was closely related to the slow translation speed of Morakot during this postlandfall period. This quasi-stationary nature of the intense convective band and the lifting effect of the terrain over land resulted in the record-breaking rainfall (Figure 2b). Thereafter, the intense convective band moved faster northward with the TC circulation (Figure 5d).

3. Unique Features of Morakot

[12] From observations, it is clear that at least two unique features of Morakot contributed to the heavy rainfall over southern Taiwan. The first was the slow translation speed of the TC, which caused a long duration of typhoon influenced

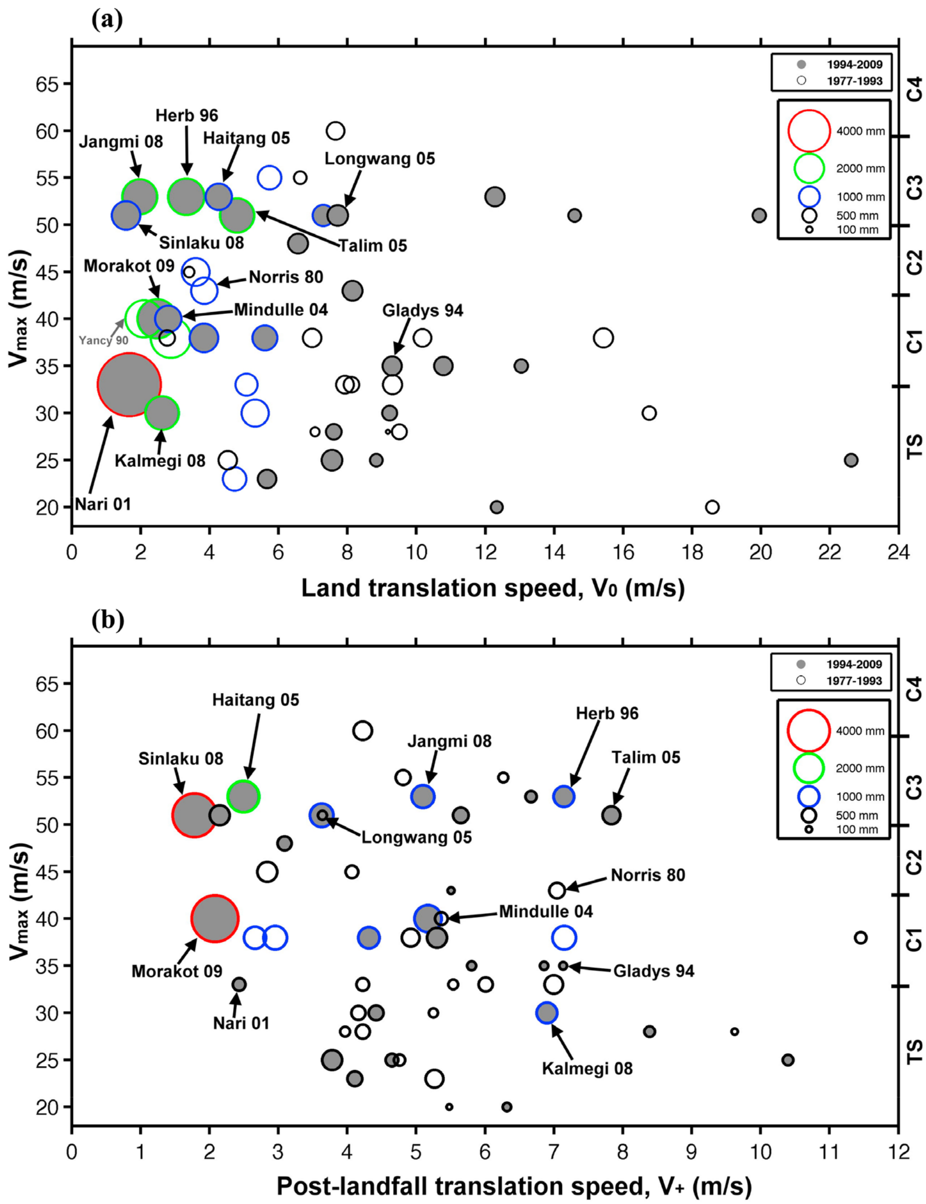

Figure 3. The total rainfall (mm) summed over the 25 CWB surface stations as a function of TC intensity (maximum wind speed) and translation speed for all landfall TCs in Taiwan from 1977 to 2009 (a) during TC landfall and (b) during the period from the TC moving over ocean to 100 km offshore (post-landfall). Names of some TCs are indicated. Rainfall is proportional to the circle size (area) with different perimeter colors (see scale in the top right corner). The TCs of the first half (1977–1993) and the second half (1994–2009) are represented by open and solid circles, respectively. Note that the range of abscissa is different for the two panels.

rainfall. The second was the strong southwesterly flow that transported moisture-laden air to the northern South China Sea (SCS) and the southern Taiwan Strait (TS). In order to examine such unique features of Morakot, we first searched for typhoons with similar tracks to Morakot before, during, and after TC landfall using the Joint Typhoon Warning Center (JTWC) best track data from 1950 to 2009. Eighteen typhoons were identified, including Longwang (2005), Talim (2005), Haitang (2005), Herb (1996), Gladys (1994), Omar (1992), Norris (1980), Billie (1976), Nina (1975), Bess (1971), Elsie (1969), Nora (1967), Clara (1967), Mary (1965), Amy (1962), Pamela (1961), Freda (1956), and Dinah (1956). The tracks of these typhoons, along with that of Morakot, are shown in Figure 6 in a chronological order with corresponding identification numbers. The tracks were relatively diverse at great distance from Taiwan, but they became similar to each other in the critical zone between 118°E and 127°E. A composite study of these 19 typhoons

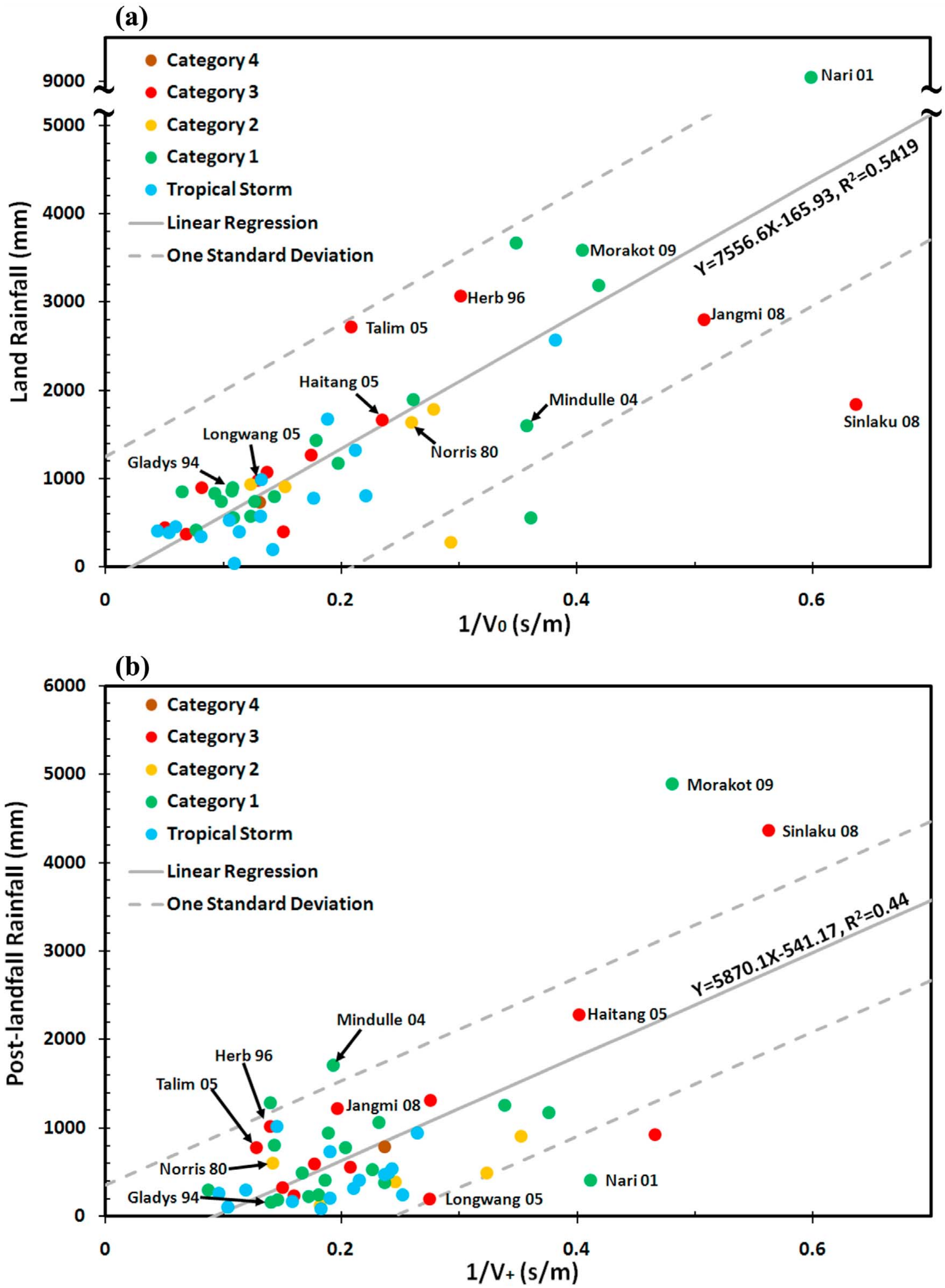

Figure 4. Same as Figure 3 but showing rainfall (mm) versus the reciprocal of TC translation speed (s m^{-1}), with colors denoting the TC intensity from tropical storm to Category 4. Gray solid line indicates the linear regression, and gray dashed line indicates the range of 1 standard deviation.

was then performed by using the National Centers for Environmental Prediction (NCEP) reanalysis data [*Kalnay et al.*, 1996; *Kanamitsu et al.*, 2002], with a horizontal resolution of 2.5° × 2.5°. In addition, the high-resolution data from European Centre for Medium-Range Weather Forecasts (ECMWF) Year of Tropical Convection (YOTC) global analysis (0.25° × 0.25°) were used for a more detailed study of the typhoon structure of Morakot.

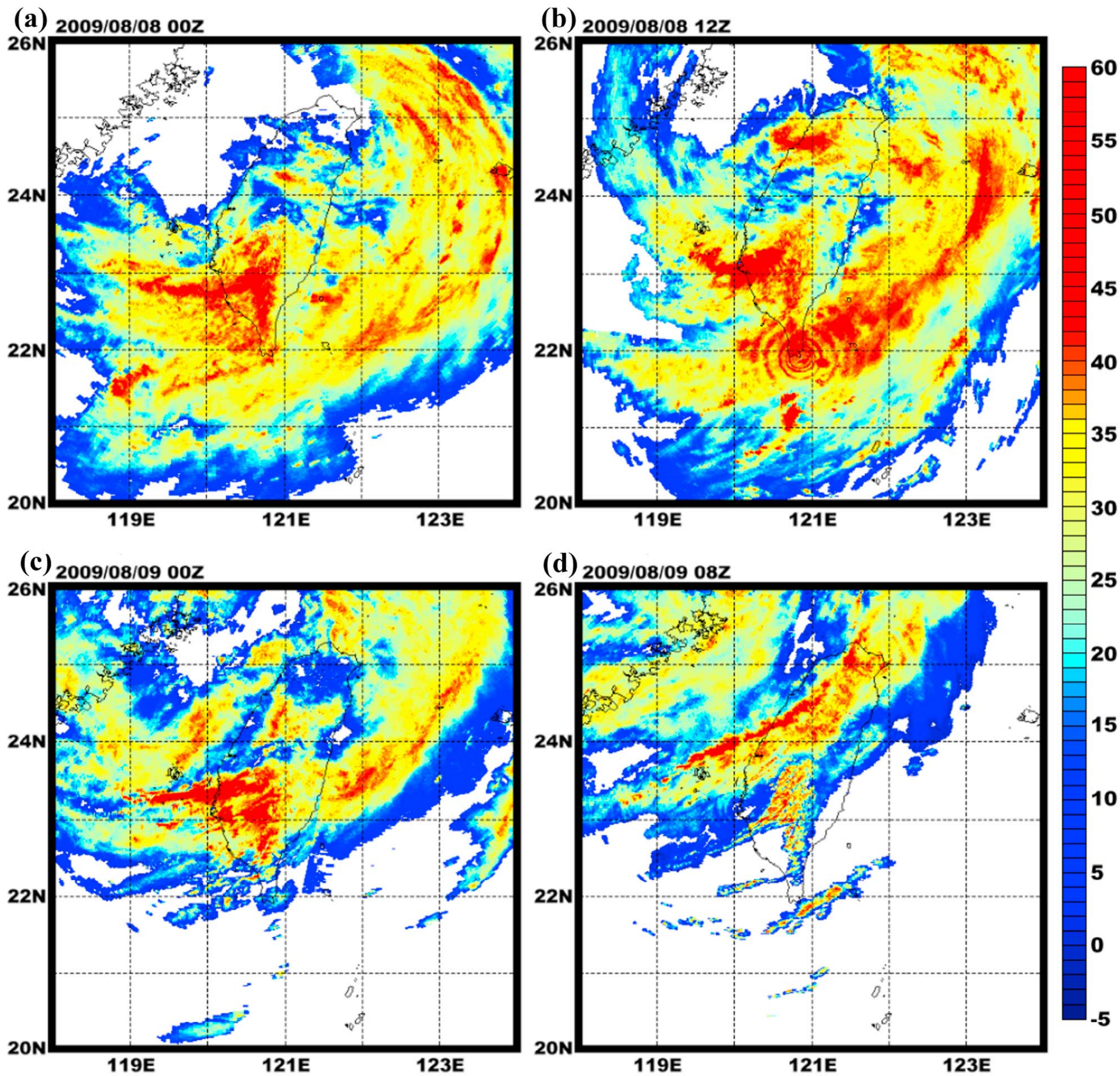

Figure 5. The CWB composite radar reflectivity (dBZ) at (a) 0000 UTC 8 August, (b) 1200 UTC 8 August, (c) 0000 UTC 9 August, and (d) 0800 UTC 9 August 2009.

3.1. Translation Speed and Southwesterly Flow

[13] Based on the track data, we computed the average translation speed at four time periods for the 19 typhoon events. The period before TC landfall was divided into two: BL1 is the period when the typhoon center was located between 124°E and 126°E, and BL2 between 122°E and 124°E. DL and AL are defined by the periods during TC landfall and within 24 h after TC center left the island, respectively. Table 1 shows that the average translation speed of Morakot in BL1 was about 23.5 km h^{-1}, and it slowed down (16.3 km h^{-1}) right before TC landfall (BL2). In DL, Morakot moved very slowly with a translation speed of 9.1 km h^{-1}. The translation speed (7.7 km h^{-1}) was even smaller in AL. These changes in the translation speeds of Morakot are very unique, as readily seen in the translation speed ratio (Figure 7a). In BL2, Marakot had dramatically reduced its translation speed to 70% of BL1. The ratio was further reduced to 40% in DL, and then about 30% in AL. Typhoon Haitang (2005) also had a significant drop in its translation speed from BL2 to DL, because it underwent a looping track before landfall [*Jian and Wu*, 2008]. The looping process, which occurred west to 122°E, was considered in DL in the calculation. Mary (1965) and Freda (1956) exhibited a continuous decreasing translation speed from BL1 to AL. However, none of these three TCs nor the others showed decreasing speed ratios comparable to those of Morakot.

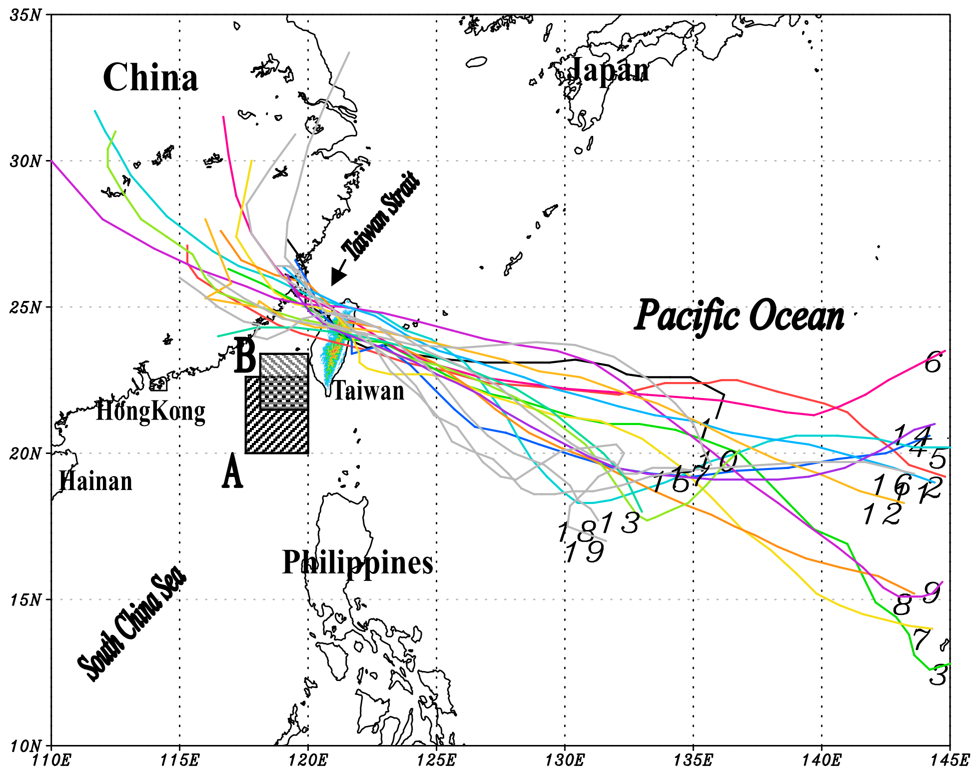

Figure 6. Tracks of 19 typhoons from the JTWC best track data, with identification numbers presented in chronological order; that is, number 1 is for Morakot (2009), 2 is for Longwang (2005), and so on. The small hatched box A denotes the rectangular area where the average winds and mixing ratio as shown in Table 2 and Figure 7 are computed. Box B is for precipitation.

[14] Another important feature of Morakot (2009) was the strong southwesterly flow that brought moisture-laden air from the tropic oceans to the southern TS. The average 850 hPa winds, mixing ratio, and precipitation rate were computed in the small areas over the southern TS (see Figure 6) during 6–42 h after TC landfall at Taiwan. The small hatched box A denotes the rectangular area corresponding to the average winds and mixing ratio, while box B refers to precipitation. The slightly different boxes were chosen because wind and moisture fields from NCEP reanalysis data were located on the 2.5° × 2.5° grid, while precipitation data were on the Gaussian grid of 1.875° × 1.875° horizontal resolution. As shown in Table 2, and more clearly in Figure 7b, the average wind speed of Morakot (21.5 m s^{-1}) was the strongest among the 19 typhoons; the second strongest was associated with Haitang (2005). The average wind directions were mostly west-southwesterly (Table 2). (Note that Gladys (1994) has a distinct wind direction from the others. The reasons are because Gladys moved very fast westward across Taiwan, weakened significantly, and became very small after passing Taiwan. The winds to the southwest of Taiwan thus turned quickly into southeasterly, instead of southwesterly, as Gladys moved away from Taiwan.) In general, this can still be referred to as "southwesterly flow," a term commonly used by the Taiwanese meteorological community. In fact, for a typhoon moving with a more northward direction like Mindulle (2004), the average flow could have a more southwesterly component [*Chien et al.*, 2008]. The average precipitation

Table 1. The Average Translation Speed (km h^{-1}) of the 19 Typhoons Before (BL), During (DL), and After Landfall (AL) at Taiwan[a]

Typhoon	BL1	BL2	DL	AL
Morakot (2009)	23.5	16.3	9.1	7.7
Longwang (2005)	26.5	26.4	25.0	20.3
Talim (2005)	19.8	21.6	21.6	23.7
Haitang (2005)	19.8	21.1	12.8	19.4
Herb (1996)	17.8	22.1	21.6	23.1
Gladys (1994)	28.6	26.6	25.5	25.0
Omar (1992)	10.6	6.8	14.3	18.0
Norris (1980)	24.1	23.3	20.4	22.4
Billie (1976)	23.0	23.8	24.8	24.8
Nina (1975)	27.8	26.3	24.6	21.9
Bess (1971)	20.3	23.4	23.7	22.2
Elsie (1969)	25.4	26.4	24.5	19.8
Nora (1967)	25.5	23.5	25.2	27.9
Clara (1967)	15.5	15.3	16.0	14.3
Mary (1965)	24.3	19.8	18.2	15.3
Amy (1962)	18.7	25.4	21.6	21.2
Pamela (1961)	28.7	30.4	29.6	26.1
Freda (1956)	19.3	15.1	12.7	11.1
Dinah (1956)	20.0	22.1	23.3	23.1

[a]The period before landfall is divided into two categories: the first (BL1) is the period when the typhoon center was located between 124°E and 126°E, and the second (BL2) was located between 122°E and 124°E. The AL represents the average translation speeds within 24 h after the TC center left the island.

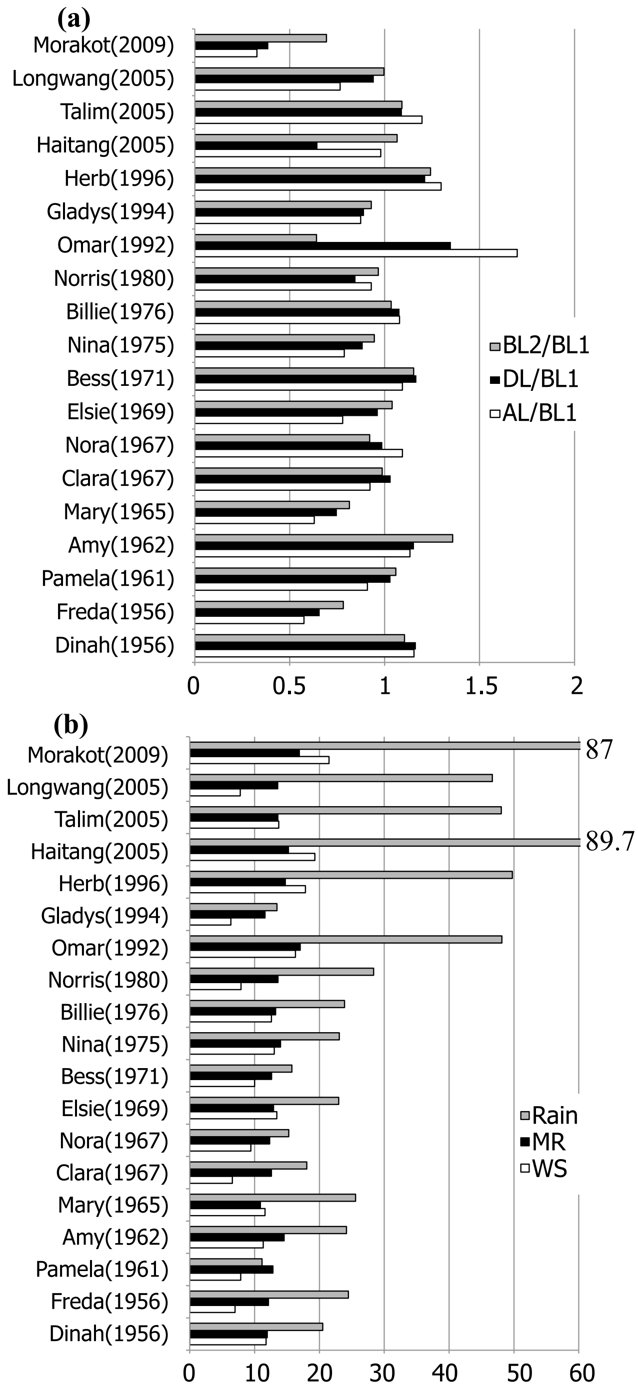

Figure 7. (a) The translation speed ratio of the 19 typhoons in the BL2, DL, and AL periods. The ratio is defined as the normalized translation speed by the speed in BL1 of the same typhoon case. (b) The average precipitation rate (mm d^{-1}), mixing ratio (MR, g kg^{-1}), and wind speed (WS, m s^{-1}) computed over the areas to the southwest of Taiwan as shown in Figure 6.

rate also indicates that Morakot and Haitang were the top two typhoons with the largest rainfall (87 and 89.7 mm d^{-1}, respectively) in the region southwest of Taiwan. This result suggests a positive correlation between wind speed of the southwesterly flow and rainfall over the southern TS when a TC passes over northern Taiwan. We therefore used the 19 pairs of data in Table 2 to compute the correlation coefficient between wind speed and precipitation. The high correlation coefficient of 0.81 confirms the abovementioned speculation. Table 2 and Figure 7b also show that a stronger southwesterly flow in the region tends to be associated with a larger water vapor mixing ratio. Their correlation coefficient was about 0.74.

3.2. Steering Flow

[15] In order to investigate the uncommonly slow translation speed of Morakot (2009), TC translation speed and direction were calculated based on the JTWC best track data between 48 h before and 48 h after TC landfall. The landfall time of Morakot (hereafter referred to as T) was defined as 1200 UTC 7 August 2009. Inasmuch as the data are only available at a 6 h interval, we used TC locations between 6 h before and 6 h after to estimate the average translation for a particular time. In addition to Morakot, the above calculations were performed for each of the other 18 TCs. The mean and standard deviation of the 19 TCs were then computed. Furthermore, NCEP reanalysis data were used to compute steering flow, including its wind speed and direction. Many different methods can be used for such task [e.g., *Chan and Gray*, 1982; *Wu and Emanuel*, 1995a, 1995b; *Jian and Wu*, 2008]. In this paper, steering flow is defined by the weighted average of winds inside an annulus between 300 and 700 km from TC center, with the weighting proportional to the distance from the center. In the vertical, pressure levels from 700 to 300 hPa were taken into account, and the average was weighted by the depth that a data point represents [*Lee et al.*, 2008]. Last, the steering flow of Morakot was also computed using the high-resolution data (0.25 degree space resolution) from YOTC.

Table 2. The Average 850 hPa Wind Speed (m s^{-1}), Wind Direction (deg), Mixing Ratio (g kg^{-1}), and Precipitation Rate (mm d^{-1}) Calculated Over a Rectangular Area to the Southwest of Taiwan During 6–42 h After TC Landfall at Taiwan[a]

Typhoon	Wind Speed	Wind Direction	Mixing Ratio	Rain
Morakot (2009)	21.5	262.8	16.9	87.0
Longwang (2005)	7.8	257.1	13.6	46.7
Talim (2005)	13.7	254.7	13.6	48.1
Haitang (2005)	19.3	265.6	15.2	89.7
Herb (1996)	17.9	252.2	14.7	49.8
Gladys (1994)	6.3	149.5	11.6	13.4
Omar (1992)	16.3	290.0	17.1	48.1
Norris (1980)	7.9	234.7	13.6	28.4
Billie (1976)	12.6	254.5	13.2	23.9
Nina (1975)	13.0	261.9	14.0	23.1
Bess (1971)	10.0	245.4	12.6	15.8
Elsie (1969)	13.4	249.3	12.9	23.0
Nora (1967)	9.4	242.7	12.3	15.3
Clara (1967)	6.6	251.0	12.6	18.1
Mary (1965)	11.6	283.6	10.9	25.6
Amy (1962)	11.3	247.2	14.6	24.2
Pamela (1961)	7.9	233.4	12.8	11.2
Freda (1956)	7.0	247.6	12.1	24.5
Dinah (1956)	11.8	250.4	12.0	20.5

[a]See Figure 6 for location: the small hatched box A denotes the area where the average winds and mixing ratio were computed, and box B is for precipitation.

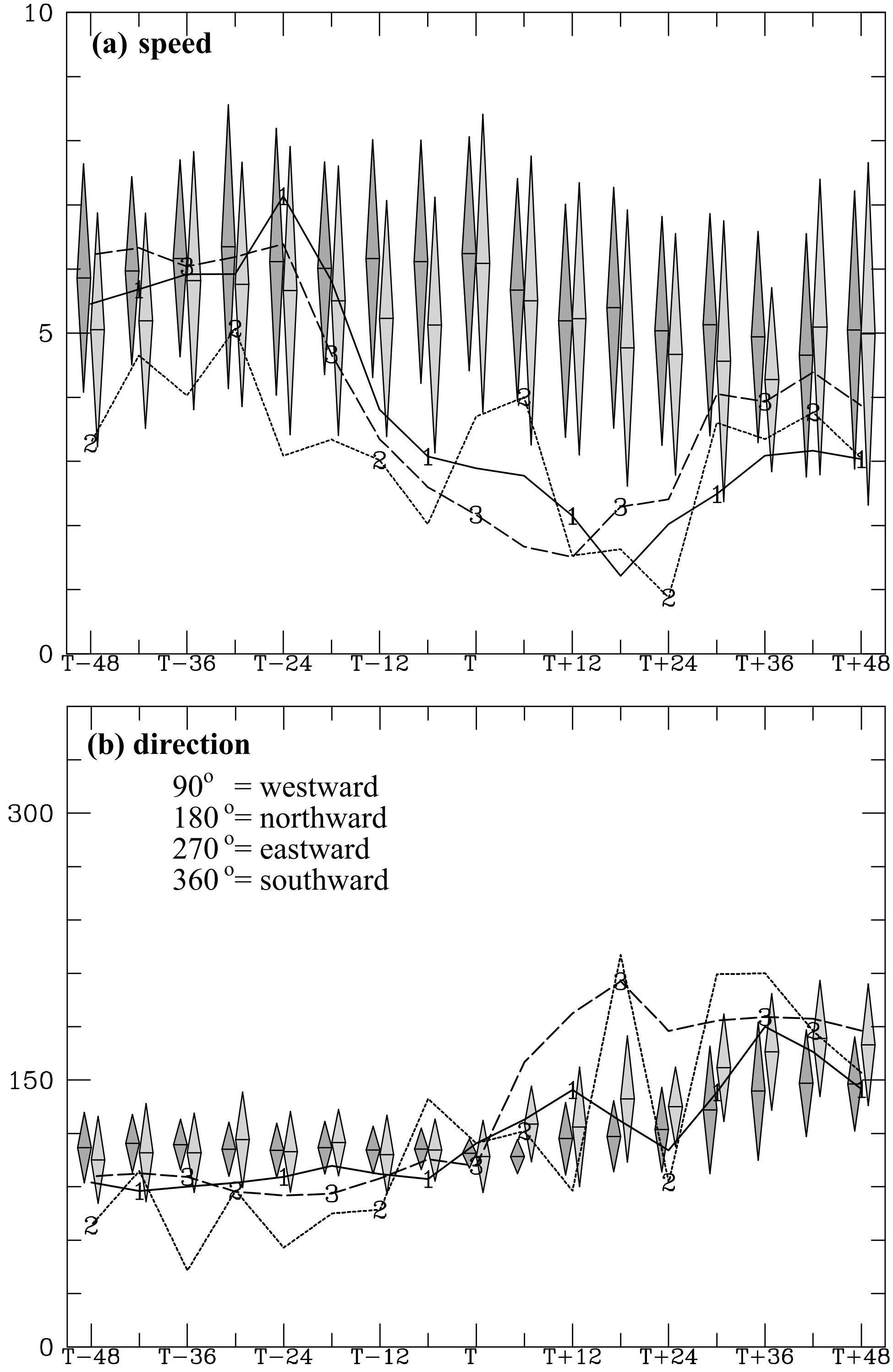

Figure 8. Curve 1 presents translation (a) speed (m s^{-1}) and (b) direction (degree) for Morakot based on the JTWC best track data from T−48 to T+48. T is the time of TC landfall. Dark shaded rhombi are similar, but showing the mean and standard deviation of translation for the 19 typhoons. Curve 2 with light shaded rhombi is the same as curve 1 with dark shaded rhombi, except for the steering flow speed and direction computed from NCEP reanalysis data. Curve 3 is the same as curve 2 but based on YOTC data.

[16] The translation speed of Morakot computed from the JTWC best track data (curve 1 in Figure 8a) was about 6–7 m s^{-1} (equivalent to 21.6–25.2 km h^{-1}) before T−24 (24 h before landfall). The speed dropped rapidly to about 3 m s^{-1} from T−24 to T, and then further to approximately 1.4 m s^{-1} (~5 km h^{-1}) at T+18. The translation speed increased slightly afterward. The translation direction of Morakot (curve 1 in Figure 8b) remained slightly over 90 degrees

(nearly westward moving) before T. After landfall, Morakot turned gradually onto a northwestward direction, except for a recurving path between T+12 and T+24. A comparison of these results on Morakot in relation to the mean and standard deviation of the 19 typhoon cases (dark shaded rhombi in Figure 8a) indicates that its translation speed before T−18 was close to the mean or at least within the range of one standard deviation. This finding suggests that Morakot's motion was like a normal westward-moving typhoon during this period. After T−18, however, Morakot started to slow down and became an outlier among the 19 typhoons until T+36. On average, these 19 typhoons showed a trend of reducing moving speed before and after TC landfall, but the speed change of Morakot was the most dramatic. As for translation direction, the mean of these typhoons (dark shaded rhombi in Figure 8b) presented a slightly more northward direction compared with that of Morakot (curve 1 in Figure 8b) before TC landfall.

[17] The steering flow speed of Morakot based on NCEP reanalysis data (curve 2 in Figure 8a) was around 4 m s^{-1} before T−30 and decreased to about 2 m s^{-1} at T−6. The calculation of steering flow might introduce some error, as seen from the fluctuation nature of the curve before TC landfall, because of the low resolution of NCEP data. In addition, when the typhoon was located near Taiwan, the flow was modulated by terrain, which could further increase computation error. The speed increase of steering flow at T and T+6 could be related to such problem. Steering flow speeds were lowest between T+12 and T+24, and increased a little thereafter. The steering flow speeds of Morakot were very small compared with the mean and standard deviation of all 19 typhoons computed from NCEP reanalysis data (light shaded rhombi in Figure 8a). Many of them were even smaller than one standard deviation from the mean. Despite some errors introduced by the low-resolution data, terrain effect, and definition of the steering flow, these results remain generally consistent with the translation speeds calculated from the JTWC best track data. A similar conclusion can also be made for the steering flow direction (Figure 8b).

[18] Since the 2.5 degree resolution of NCEP reanalysis data was relatively low for the steering flow calculation of Morakot, YOTC 0.25 degree data were used to perform the same computation. Figure 8a shows that with about 100 times more grid points utilized in the calculation, the steering flow speeds based on YOTC data (curve 3) agreed more closely with translation speeds (curve 1), except for approximately a 6 h lead time, than those of NCEP reanalysis data (curve 2). The lead time was reasonable because the steering flow speed was computed instantaneously at each 6 h, and its influence on the TC movement could only be observed 6 h later. This suggests that the method of steering flow computation in this study is capable of forecasting typhoon movement. However, one shortcoming of this method deals with steering flow direction from T+6 to T+30 (curve 3 in Figure 8b). During these times, steering flow direction manifested a more northward component compared with the translation direction from the JTWC best track data. This could be related to terrain interference because the same trend was also observed in NCEP reanalysis data (curve 2 at T+18). Nonetheless, before TC landfall, the steering flow directions were very consistent with translation directions. It is therefore evident that the unique translation speed of Morakot (2009) was closely related to the slow steering flow provided by the surrounding environment.

[19] It is noted that the mean translation speed (dark shaded rhombi) was generally faster than the mean steering flow speed computed from NCEP reanalysis data (light shaded rhombi), especially during the westward-moving course of the TCs (Figure 8a). This is consistent with the finding of *Carr and Elsberry* [1990] who pointed out that a westward-tracking TC in general moves faster than the steering flow in the Northern Hemisphere. However, our results do not overwhelmingly agree with their other conclusions, particularly on the tendency of TCs to move to the left of the steering. In several of time periods before T the mean translation direction was larger than the mean steering direction (Figure 8b). Nonetheless, these differences do not seem to appear in the steering flow calculation from the high-resolution data set because the YOTC steering flow (curve 3) was in better agreement with the observed translation (curve 1) for the Morakot case than the NCEP (curve 2).

4. The Composite Results

[20] The slow steering flow caused Morakot to move with an uncommonly slow speed around Taiwan. It is therefore important to examine the difference of the environmental flow between Morakot and the other typhoons with similar tracks. We used NCEP reanalysis data to perform composite analyses by taking an average of meteorological fields for all the 19 typhoon cases and then compared the fields with those of Morakot. The composite 700 hPa geopotential height, winds, and relative humidity (Figure 9a) show that at T−24, the TC center was located east of Taiwan and the PSH extended westward from southern Japan to east China. The composite TC tended to move westward because of the steering effect dominated by the PSH. Morakot, which was then located east of Taiwan, had lower central pressure, larger relative humidity, and stronger winds than the composite (Figure 9b). To the west near Hainan (see Figure 6 for location), there was another low-pressure area associated with Typhoon Goni (2009). The PSH extended toward the northwest from Japan to northeast China, which was very different to the composite. The difference between Morakot and the composite (Figure 9c) shows that relatively low pressure occupied the WNP. In addition to Goni that was located to the west of Morakot, another low-pressure system that later developed onto the third typhoon (Etau 2009) in this nearby small area presented itself to the east of Morakot. A positive pressure anomaly with a maximum of ~100 gpm over northeastern China and a negative anomaly to its east reflected the northwestward extension of the PSH and the southward extension of an MLT, respectively, which rarely occurred in the 19 selected cases (Figure 9b).

[21] At later times (T-12) the difference between Morakot and the composite (Figure 10a) shows that Morakot had moved very close to the east coast of Taiwan and both the low centers of Etau and Goni had deepened slightly. The positive pressure anomaly continued to occupy northeastern China. The steering effect that normally causes a typhoon to move westward, as shown in the composite, did not exist because of the northwestward extension of the PSH and the

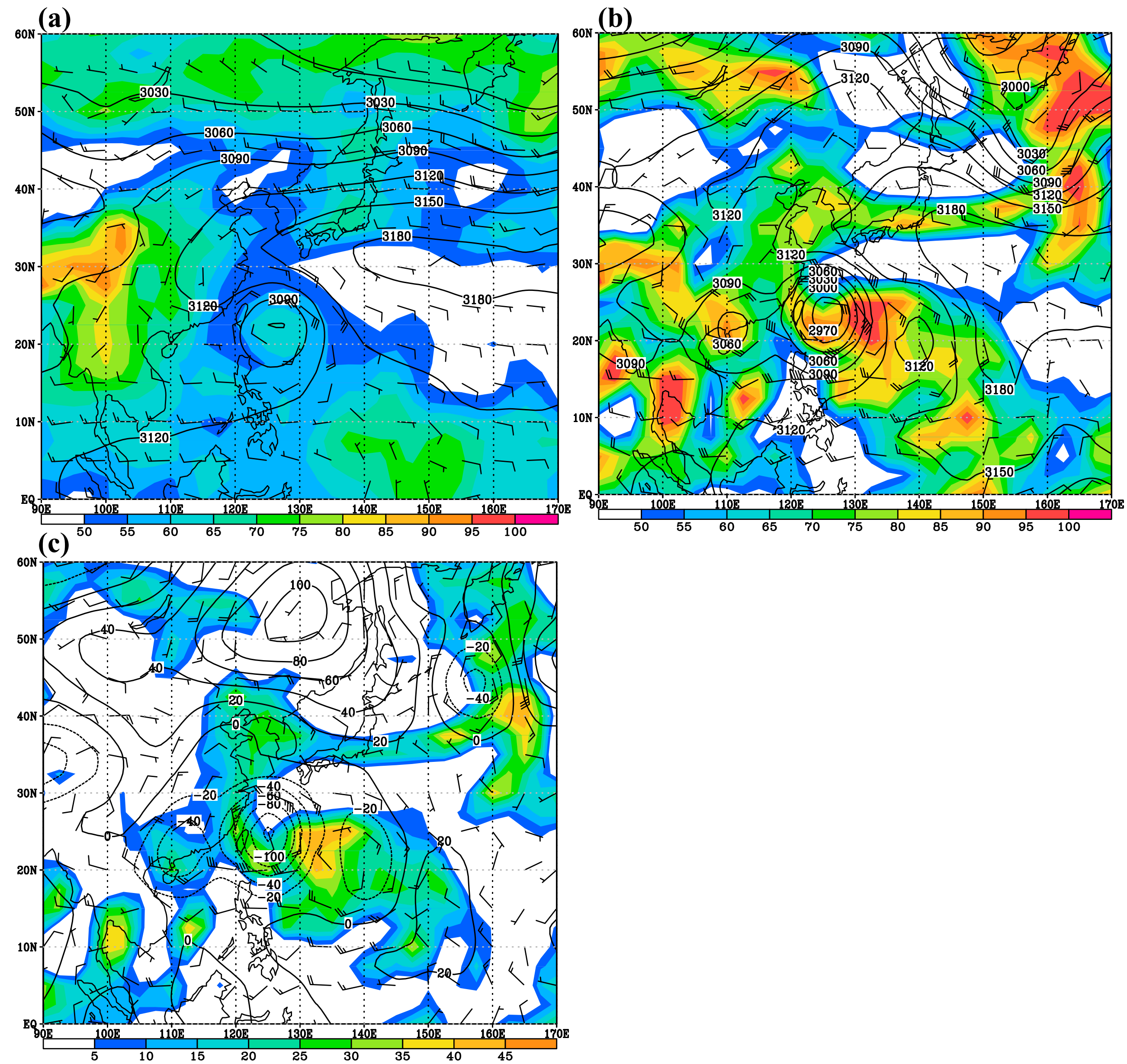

Figure 9. The 700 hPa geopotential height (contour lines at a 30 gpm interval), RH (shading with scale shown at bottom), and winds (full barb = 5 m s^{-1}; half barb = 2.5 m s^{-1}) at T−24 for (a) the composite and (b) Morakot. (c) The difference between Morakot and the composite, with solid lines (20 gpm interval) denoting zero or positive difference and dashed lines denoting negative difference.

low-pressure systems surrounding Morakot. This particular environment resulted in the weak steering flow and the translation speed change in the Morakot case, as seen in Figure 8. At the landfall time of Morakot (Figure 10b), both low pressure of Morakot and Goni weakened slightly. There was large positive RH anomaly in the southwest and the east sections of the Morakot circulation. At T+12 and T+24 (Figures 10c and 10d), the low pressure of Etau deepened and the three typhoon centers appeared to rotate connectedly in a counterclockwise direction along an axis. Located in the center of the axis, Morakot moved with a very slow speed after landfall. The positive RH anomaly extended all the way from the eastern Bay of Bengal to southern Taiwan at T+24. Another important feature of the Morakot case is the positive and negative height anomalies in the midlatitudes, which were nearly stationary within 48 h. This result reflects the persistently northwestward extension of the PSH, creating a favorable condition for weak steering flow to slow down Morakot.

[22] Besides the midlatitude influences, the above results also show that Typhoons Goni and Etau (about 3000 km apart) created a unique environment for Morakot to become a nontypical TC that was embedded in a large-scale convection region with a monsoon circulation of different time scales in the tropical WNP. *Hong et al.* [2010] pointed out that this large area of cyclonic circulation (so-called monsoon gyre), which was related to a submonthly wave pattern during the cyclonic phase of the intraseasonal oscillation,

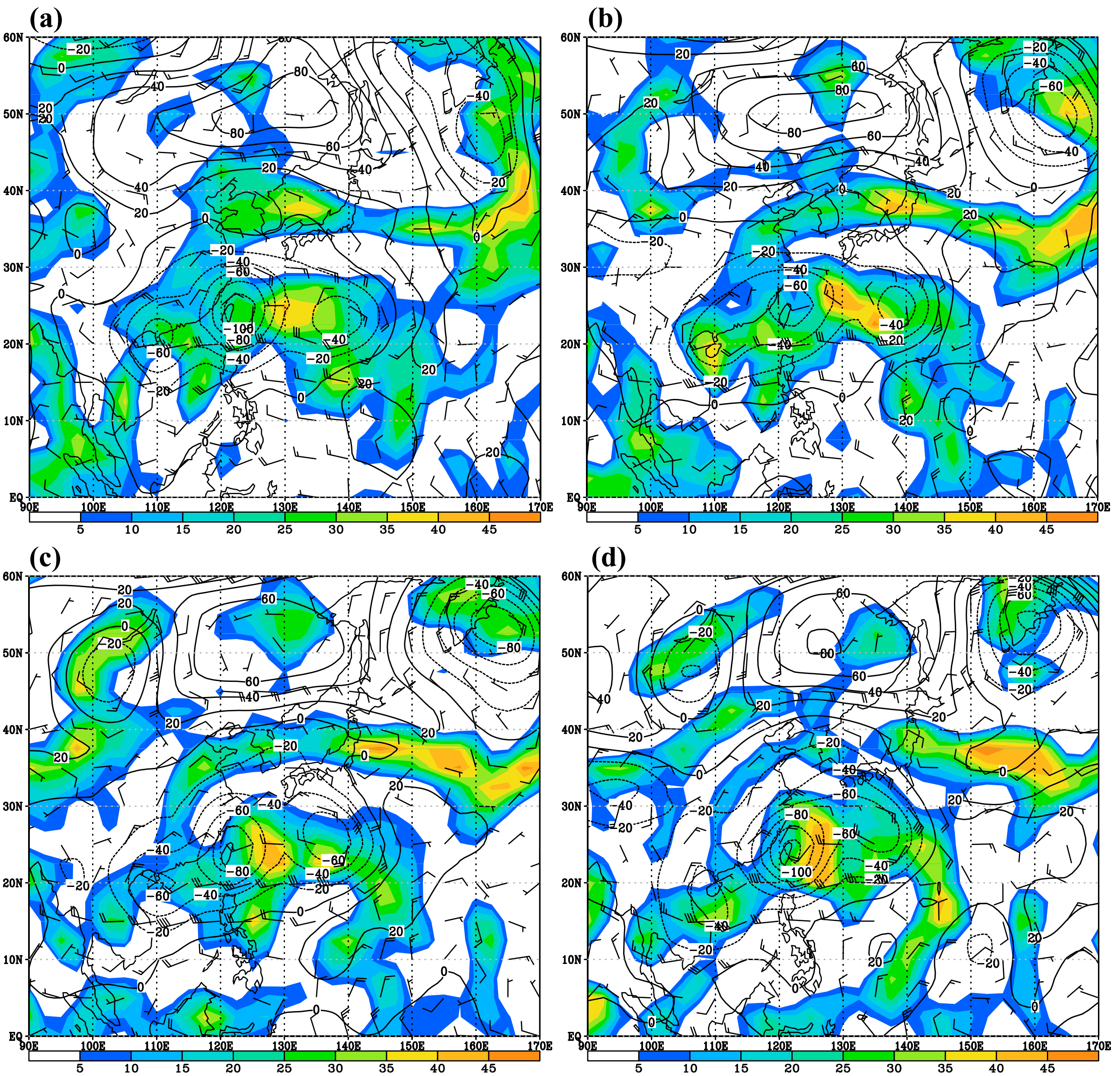

Figure 10. Same as Figure 9c but for times at (a) T−12, (b) T, (c) T+12, and (d) T+24.

and the topographic lifting effect of steep terrain resulted in the record-breaking rainfall in southern Taiwan. An important question, however, is what the role of this monsoon gyre is in determining the translation speed. The answer lies in the comparison between Figures 8 and 10, which show that Morakot's translation speed dropped significantly from T−18 to T+24 while during the same period the three TCs were rotating in a counterclockwise fashion. Although the TCs were farther apart than the traditional distance of having the Fujiwhara effect, the interaction of their circulation was still very important in causing the translation speed change of Morakot within this large-scale monsoon circulation.

[23] At T+24, the composite TC center had passed Taiwan and was making landfall on the southeast China coast (Figure 11a) while Morakot remained near northwestern Taiwan (Figure 11b). Although the 500 hPa plots show a large-scale pressure pattern similar to those at 700 hPa, they provide additional synoptic-scale insight. The 5880 gpm contour line of the PSH composite pattern almost reached the east China coast at this time, but in the Morakot case it only extended to Japan. This ridge of the PSH extended northwestward except for a slight interference by a small trough. There was also a southwestward extension of the PSH, as evidenced by the 5880 gpm contour line in Figure 11b and the positive pressure anomaly in Figure 11c. The buildup in this part of the ridge additionally contributed to the northwestward movement of Morakot at a later time. Figure 11 also shows another MLT moving eastward (see Figure 10 as well) from northern China toward northeastern China between T and T+24.

[24] In order to examine low-level flow and moisture structures, the plots at the 850 hPa level were chosen for T+36.

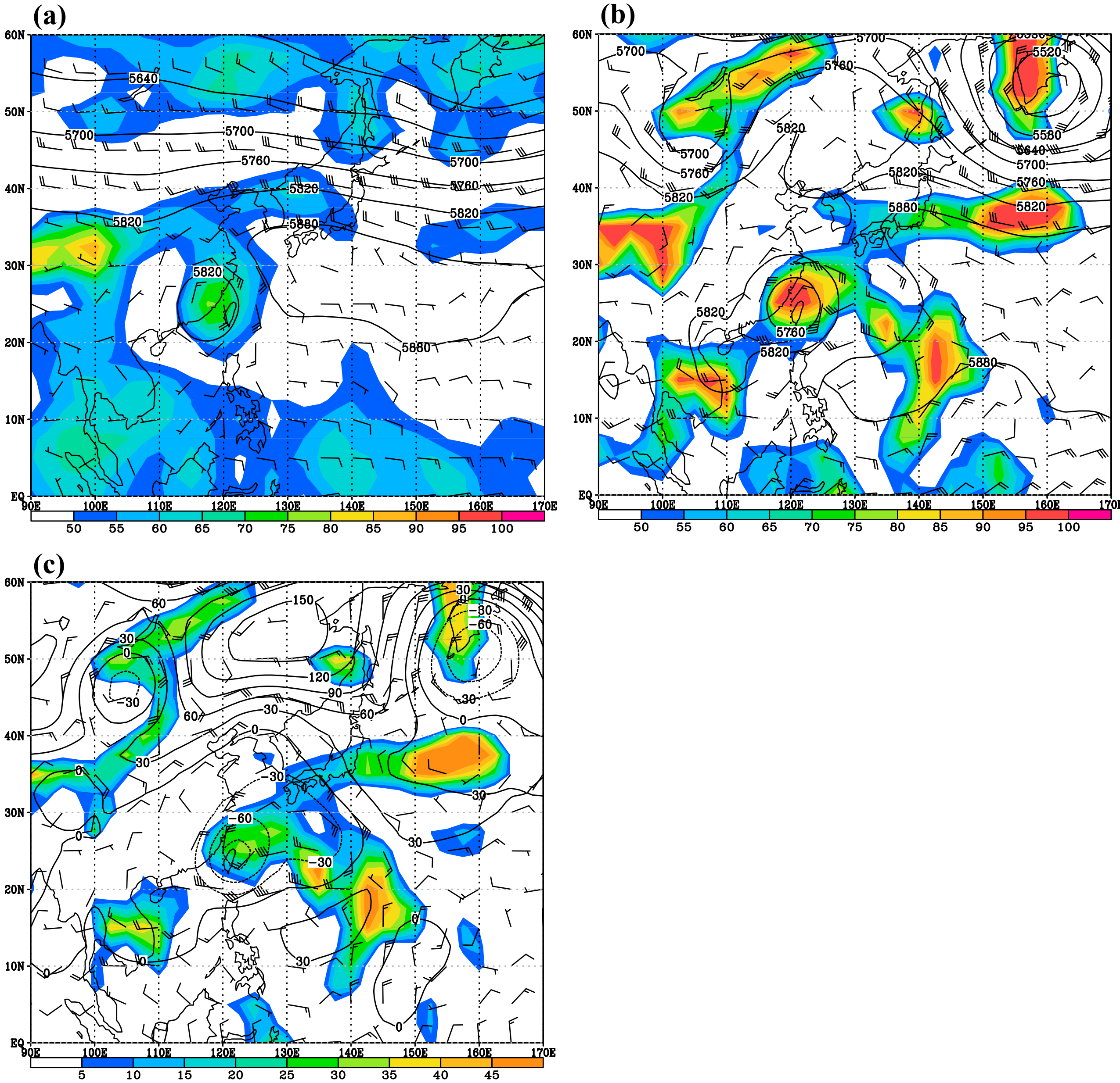

Figure 11. Same as Figure 9 but for the 500 hPa level at T+24.

At this time, Morakot was located over the ocean northwest of Taiwan (Figure 12b). The composite TC center, however, had moved inland over southeastern China (Figure 12a). A low center of ~1380 gpm, representing the aforementioned MLT over northern China at 500 hPa, had moved eastward to ~110°E (Figure 12b). The PSH continued to extend toward the northwest, but the midlatitude ridge was weakened by the approaching MLT from the west. The difference (Figure 12c) shows that the negative anomaly of the low-pressure systems surrounding Morakot extended toward the north/northwest to merge with the MLT. This pressure change, along with the positive anomaly to the southeast resulting from the PSH, created an environment for Morakot to move northwestward with a slight increasing speed. Figure 12b also shows that with Morakot moving northwestward, a southwest-northeast-oriented zone of strong moist southwesterly flow (about 15–25 m s^{-1}) extended from the eastern Bay of Bengal all the way toward southwestern Taiwan. This moisture conveyor belt, which is readily seen in Figure 12c, played an important role in the heavy rainfall over southern Taiwan because it transported moisture-laden and unstable air toward Taiwan, resulting in the MCS that produced heavy rainfall over land.

5. High-Resolution Analyses

[25] High-resolution (0.25° × 0.25°) data from YOTC is used to further study the typhoon structure that influenced the steering flow of Morakot. In addition, the moisture and winds of the southwesterly flow associated with Morakot are examined.

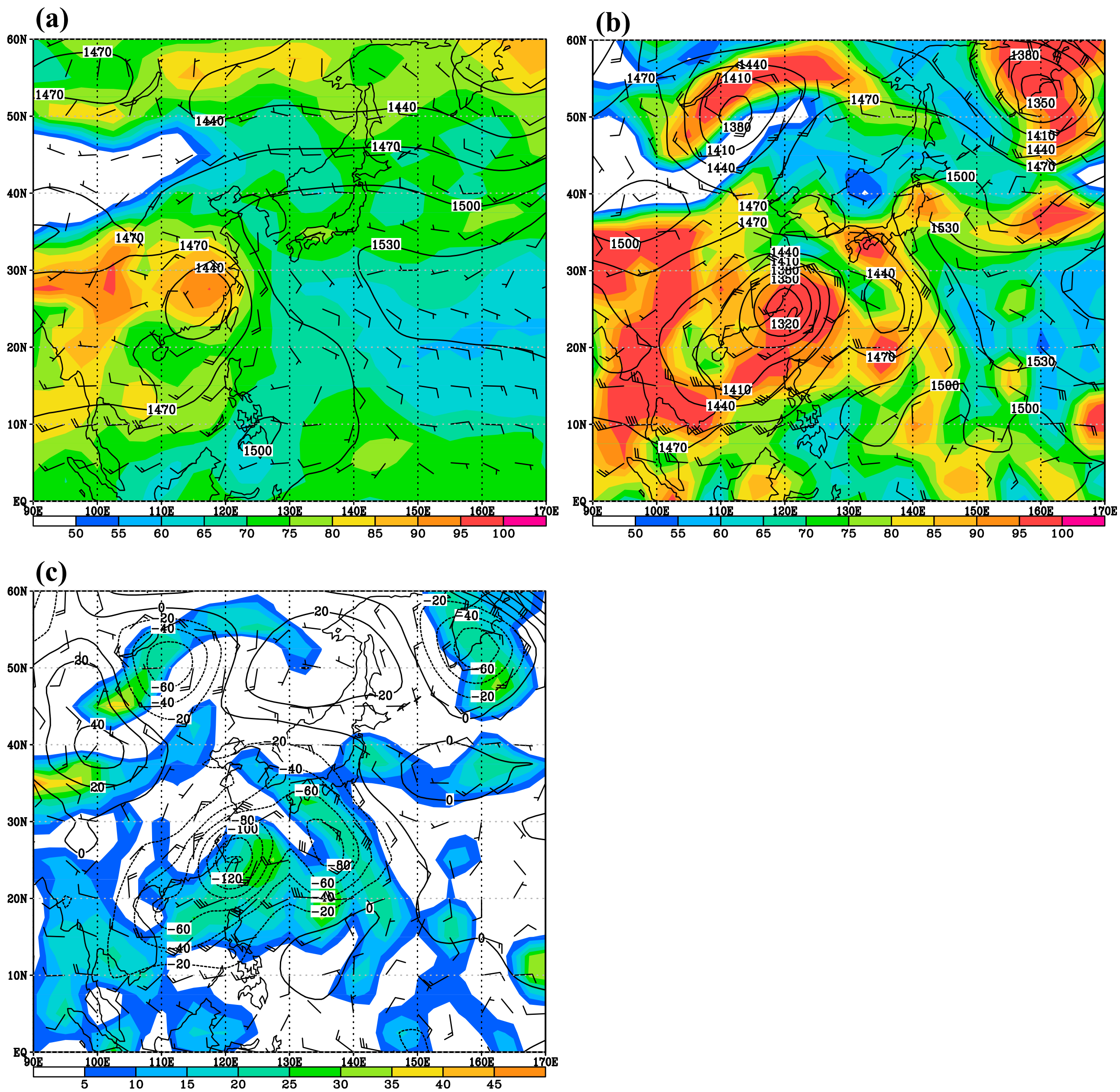

Figure 12. Same as Figure 9 but for the 850 hPa level at T+36.

5.1. Typhoon Structure That Influences the Steering Flow

[26] Since the steering flow computed from the YOTC data agrees well with the observation (as seen in Figure 8), we further examine the causes of the steering flow change using this data set. We first analyze the average steering flow at 5 individual levels (i.e., 700, 600, 500, 400, and 300 hPa). As seen in Figure 13 the steering flow at lower levels, such as 700 and 600 hPa, did not change much between T−54 and T+54. At 500 hPa, the steering flow changed from easterly before T−12 to southerly after T+6 with persistently slow speeds. The primary change that caused a significant translation speed drop from T−24 to T+18 (Figure 8) occurred at the upper levels, including 400 and 300 hPa. At these levels, the steering flow was strong (~10 m s^{-1}) and nearly easterly at times before T−24. Subsequently, the 400 hPa flow weakened which was followed by a flow reduction at 300 hPa. In addition to the speed change, the steering flow gradually turned southerly after Morakot made landfall in Taiwan.

[27] The abovementioned wind changes are more easily seen in Figures 14a and 14b, which present flow evolution in the u and v components, respectively. At 700 hPa, the u-component steering flow was very weak and varied from about −2 to 2 m s^{-1} (Figure 14a). The easterly flow increased with height at early times with a maximum speed around 10 m s^{-1} at 400 and 300 hPa. After T−24, the easterly flow weakened rapidly, especially at upper levels. By T+12, the u-component steering flow approached a very slow speed being relatively consistent among the 5 layers in

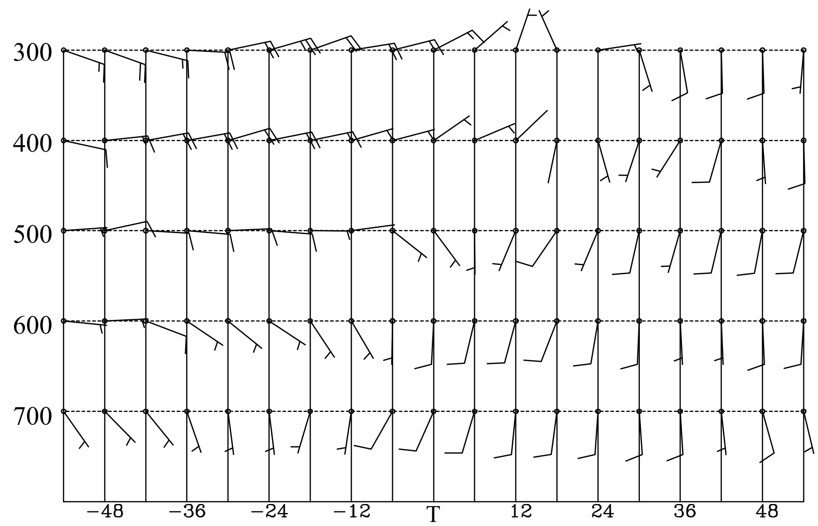

Figure 13. The steering flow at 5 levels (700, 600, 500, 400, and 300 hPa) from T−54 to T+54 at a 6 h interval, with T being the TC landfall time. The speed and direction of steering flow (full barb = 5 m s^{-1}; half barb = 2.5 m s^{-1}) are plotted in the format of the station model.

the vertical. The v-component steering flow was relatively weak throughout the entire period (Figure 14b). Upper-level northerlies were nearly counteracted by low-level southerlies before T, resulting in a steady westward to west-northwestward direction of Morakot before landfall. After T, the upper-level v-component flow gradually switched to southerly. Along with the slight increase in the low-level flow, this change caused Morakot to turn northwestward after passing Taiwan.

[28] In order to investigate the cause of these changes, we further divided the steering flow calculation into two parts, the northern (NTC) and southern half sections (STC) of the TC. Specifically, the two average regions were defined by dividing the 300–700 km annulus into half from east to west through the TC center. Figures 14c and 14d present the u-component steering flow averaged in the NTC and STC, respectively. Comparison of these diagrams clearly indicates that the flow in the NTC contributed to the westward steering and rapid flow reduction after T−24. In the STC, the u-component steering flow was westerly at 500–700 hPa. Along with the easterly in NTC, this indicates that the typhoon circulation had a relatively symmetric structure at lower levels. At upper levels (400 and 300 hPa), however, the typhoon was quite asymmetric in terms of the u-component steering flow before T−24 because of the lack of westerlies in the STC; instead, easterly flow was found. Such large differences in the vertical caused a very small u-component steering flow in this region, resulting in the dominance of the easterly steering by the NTC circulation. After T−24, the upper-level easterlies started to decrease and became westerly at a later time. This change, combined with the reduction of the u-component steering flow in the NTC, resulted in the weakening of the westward steering. Therefore, there were two factors that influenced the steering flow of Morakot at 300 and 400 hPa. First, in the NTC, the easterly steering flow weakened consistently over the entire layers after T−24. Second, the upper-level flow in the STC changed from easterly to westerly.

[29] With the abovementioned findings, it is therefore necessary to compare the flow at upper and low levels. The 300 and 700 hPa levels at T−24 and T are chosen for discussion (Figure 15). The 300 hPa geopotential height analysis shows tight height gradients in the NTC and weak gradients in the STC at T−24 (Figure 15a). The trough associated with the TC extended far to the south. This resulted in mostly strong easterlies in the NTC circulation and diverse wind directions, but generally an easterly wind component in the STC. To the north of the TC, the PSH weakened and a short-wave trough approached from the west at T, as evidenced by the 9780 and 9750 gpm contour lines (Figure 15b). This short-wave trough which occurred in between the aforementioned two MLTs appeared only at levels above ~500 hPa. In addition, a low-pressure center that was associated with the northwestward-tilting Etau appeared to the east-northeast of Morakot. These pressure patterns caused the weakening of the pressure gradient and the easterly winds in the NTC. Pressure increased to the south of the TC around the Philippines within the past 24 h, resulting in a more circular circulation in the STC. This explains why the 300 hPa u-component steering flow turned from easterly to westerly in this region after TC landfall (Figure 14d).

[30] The typhoon circulation was more symmetric at 700 hPa (Figures 15c and 15d) compared with that at 300 hPa. The strong easterly wind component in the NTC was thus nearly in balance with the strong westerly in the STC (see curve 1 in Figures 14c and 14d), resulting in weak easterly steering at early times and weak westerly between T−24 and T+24 (Figure 14a). Moreover, the 700 hPa winds in the eastern half of the TC in general manifested a slightly stronger southerly component than the northerly in the western half at T−24, owing to the influence from Goni. However, the scenario was reversed at 300 hPa because of the existence of Etau in the east, resulting in the cancellation of total steering in the v component before T (Figure 14b). After T, with airflow associated with TC becoming more

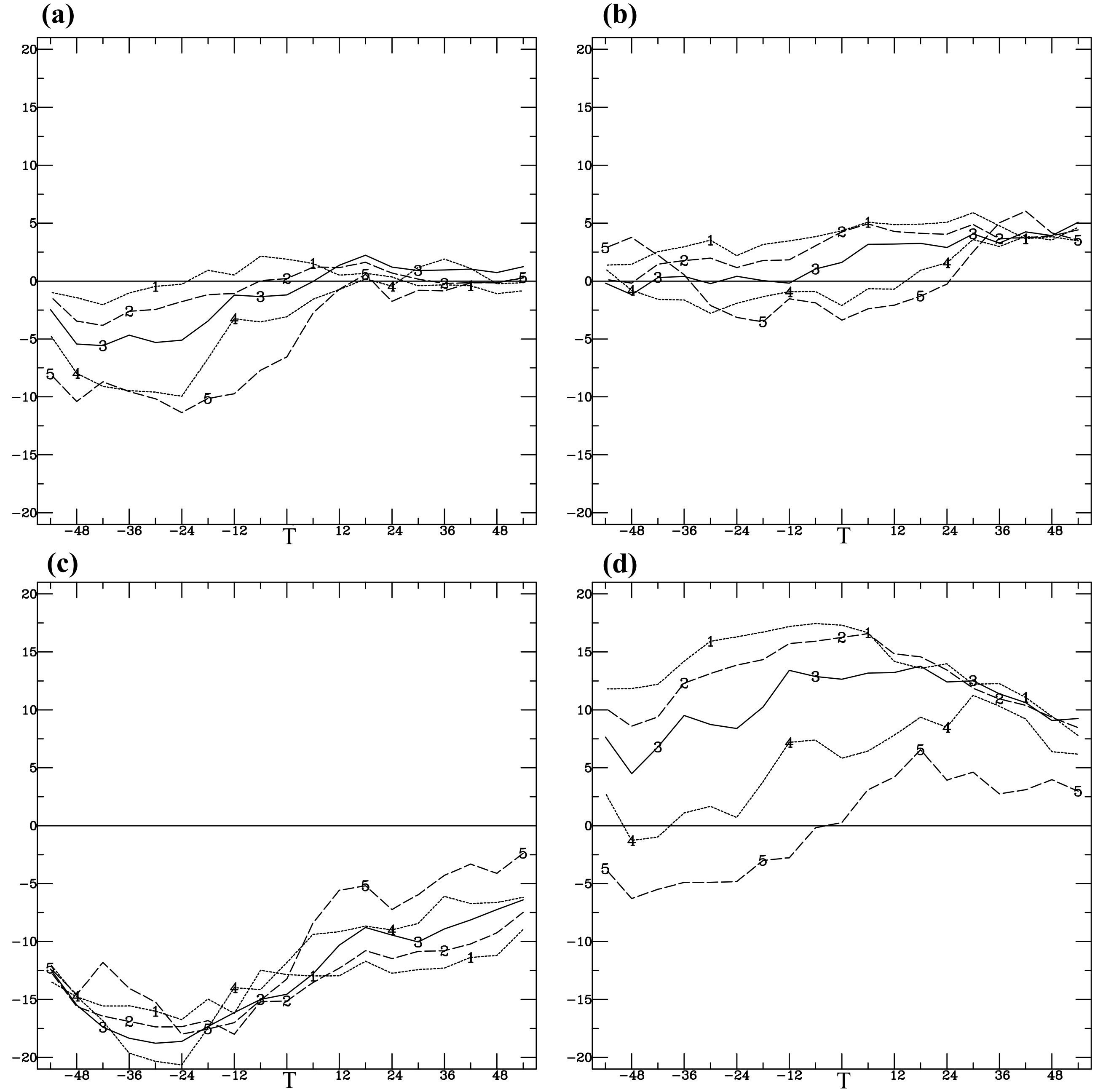

Figure 14. The (a) U and (b) V components of steering flow (m s^{-1}) at 5 levels (curves 1, 2, 3, 4, and 5 represent 700, 600, 500, 400, and 300 hPa, respectively). Times are at a 6 h interval from T−54 to T+54, with T being the TC landfall time. (c) The u-component steering flow averaged for the northern half of typhoon circulation (NTC). (d) Same as Figure 14c but for the southern half (STC).

symmetric and the dissipation of Etau at upper levels (e.g., 300 and 400 hPa), the northerly component of the steering flow weakened and turned southerly after T+24. It is therefore evident that besides the influence of the PSH and the short-wave trough, the two TCs surrounding Morakot were also very important in determining the steering flow of Morakot.

5.2. Moisture Flux

[31] The 850 hPa geopotential height, water vapor mixing ratio, and wind vectors from YOTC analysis data are presented in Figure 16. Morakot, associated with strong symmetric circulation, was located about 150 km east of Taiwan at T−12 (Figure 16a). However, moisture was not symmetric, with larger water vapor mixing ratio in the west portion of the typhoon than in the east. Winds over the southern TS were weak northwesterly. Farther to the southwest near Hong Kong, there was a northwest-southeast-oriented zone of high mixing ratio air that was associated with Typhoon Goni. Twenty-four hours later at T+12, Morakot moved slowly northwestward in northern Taiwan, with moisture-laden air covering the entire island (Figure 16b).

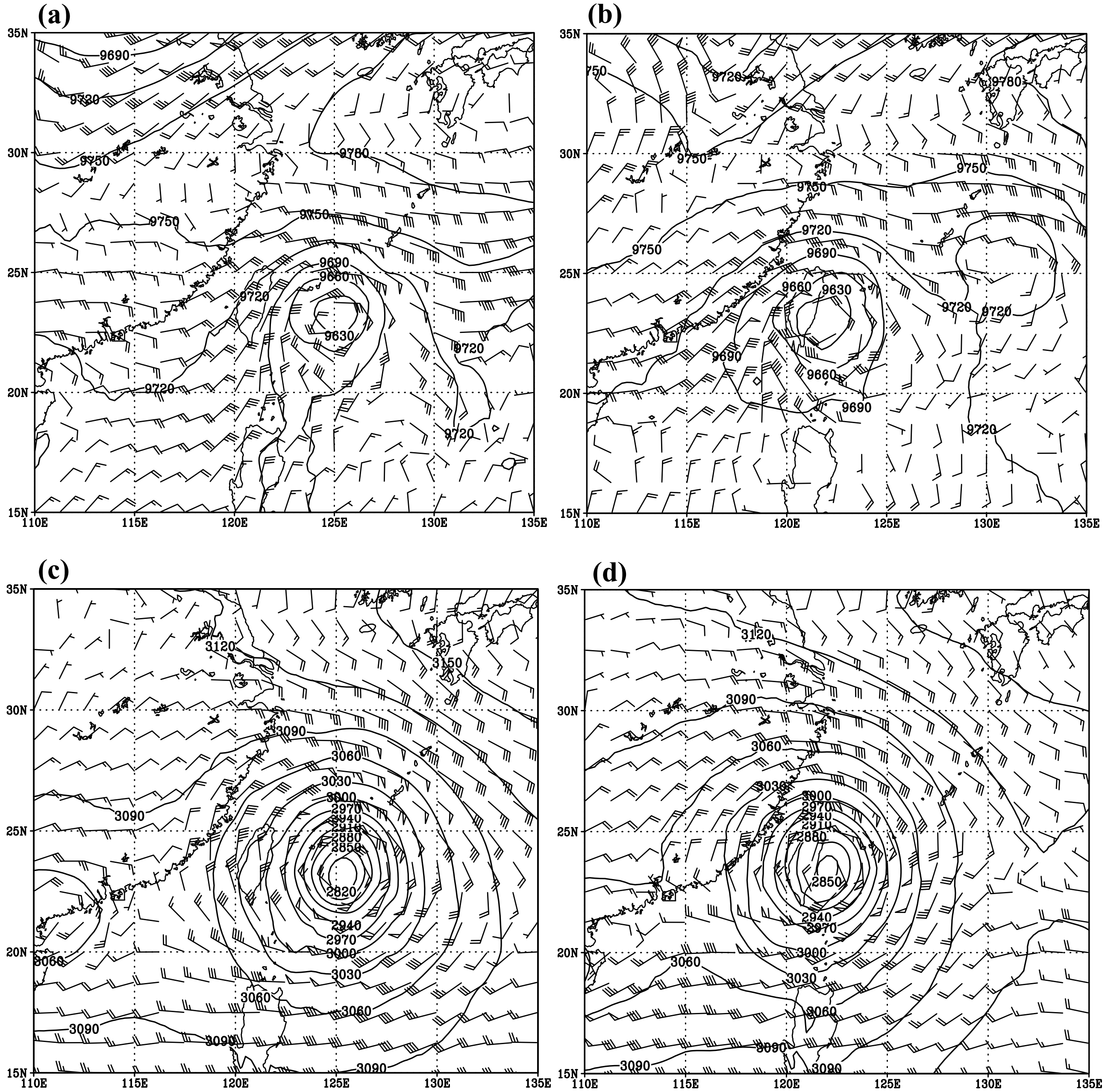

Figure 15. The 300 hPa geopotential height and winds (full barb = 5 m s^{-1}; half barb = 2.5 m s^{-1}) at (a) T−24 and (b) T. (c and d) The same as Figures 15a and 15b but for 700 hPa. Contour lines are geopotential height at a 30 gpm interval.

Over the southern TS, an east-west-oriented moisture zone extended from southern China toward southern Taiwan. Two air sources were responsible for the moisture transport, namely, northwesterly flow of the typhoon circulation and southwesterly flow that transported the moisture associated with Goni toward the east-northeast. The zone was wider in the west end than in the east, implying that strong moisture convergence occurred in this region. This can be clearly seen in Figure 17a, which shows two areas of large low-level moisture flux convergence in the southern TS. The northern part was associated with the TC circulation, and the southern part was related to the aforementioned moisture zone. These large moisture fluxes were all directed toward southern Taiwan where a huge low-level moisture flux convergence was already occurring over the mountains and low plains. This pattern agreed well with the mesoscale convective line shown in the radar observation (Figure 5b). By comparing Figures 16a and 16b, it is evident that the typhoon circulation has merged with the southwesterly flow in the southern TS and the northern SCS after TC landfall. This explains the presence of large low-level moisture flux in this region, apart from the areas of direct TC influence

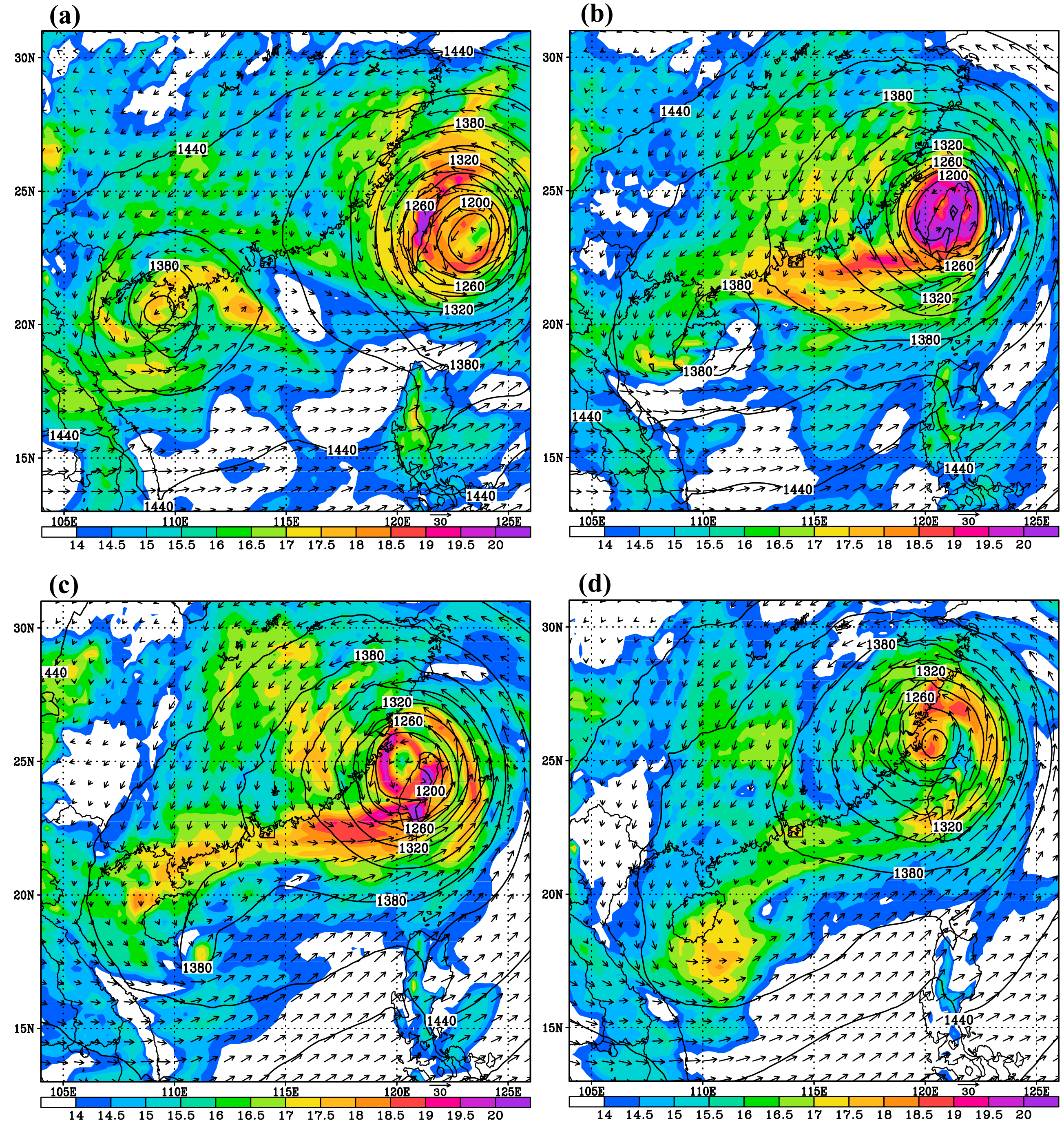

Figure 16. The 850 hPa geopotential height (contour lines at a 30 gpm interval), water vapor mixing ratio (g kg^{-1}, shading with scale shown in bottom), and wind vector (m s^{-1}, with scale shown in bottom) at (a) T−12, (b) T+12, (c) T+24, and (d) T+36.

(Figure 17a). *Ge et al.* [2010] attributed the increase of the southwesterly flow after Morakot's landfall to the mechanism of Rossby wave energy dispersion, as suggested by other studies such as those by *Ge et al.* [2008] and *Carr and Elsberry* [1995]. They pointed out that the energy dispersion by both the monsoon gyre and Morakot induced an anticyclonic circulation to its southeast side, which further enhanced the southwesterly flow through the enhanced pressure gradient.

[32] At T+24, Morakot had moved over the northern TS (Figure 16c). The zone of high humidity, this time with a greater width, remained over the southern TS. The trough of Morakot extended toward the southwest, as evidenced by the 1380 gpm contour line, which was primarily contributed by the weakening flow of Goni. This low-pressure region could further enhance the southwesterly flow to the south. The continuous supply of moist air from the west and the west-southwest resulted in strong convection and heavy

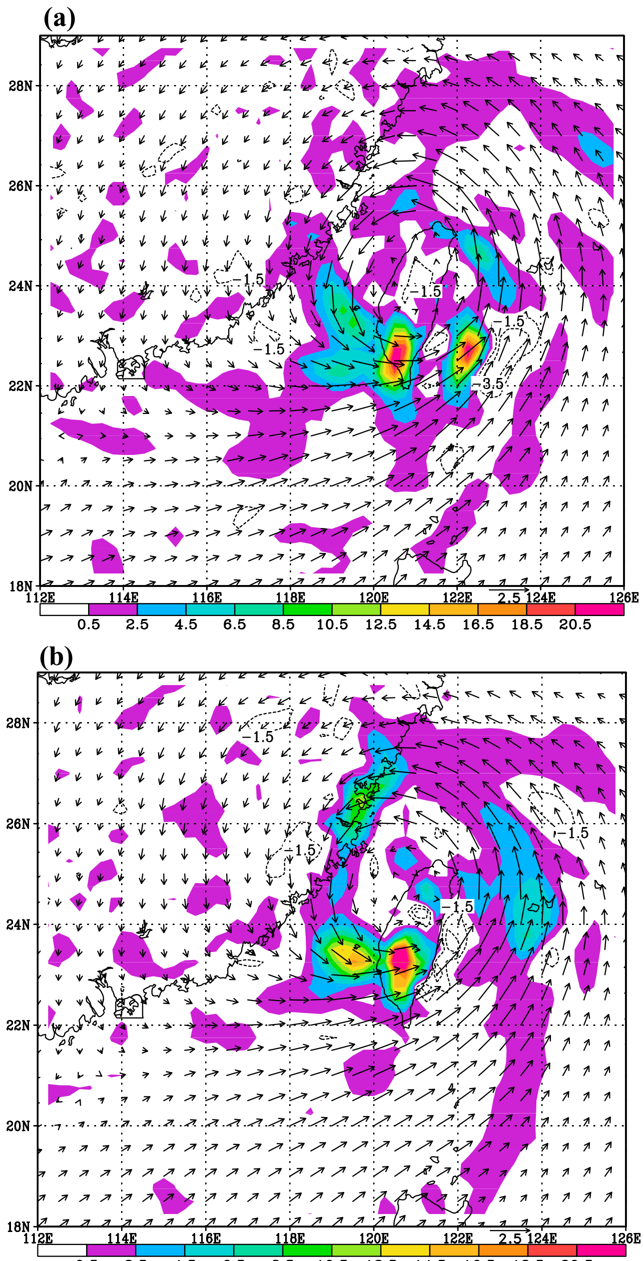

Figure 17. Moisture flux (vector) and moisture flux convergence (shading, positive) integrated over the low atmosphere from 1000 to 700 hPa at (a) T+12 and (b) T+24. The units of integrated moisture flux and moisture flux convergence are 10^3 kg m^{-1} s^{-1} and 10^{-3} kg m^{-2} s^{-1}, respectively, with scales shown at bottom and lower right. Dashed lines denote negative moisture flux convergence.

precipitation over southern Taiwan. Figure 17b shows that the two large moisture flux convergence zones had combined and became a single zone of even stronger convergence in the southern TS. This, along with the large moisture flux convergence over land, indicates that the convection and precipitation would continue in southern Taiwan. By T+36, the water vapor mixing ratio had significantly reduced over the southern TS and southern Taiwan (Figure 16d). Rainfall, however, persisted (albeit weaker) until T+48 or so.

6. Summary

[33] This paper presents composite and high-resolution analyses of Typhoon Morakot (2009), a devastating typhoon that produced torrential rainfall and brought severe damages in southern Taiwan in 7–9 August 2009. The study, primarily based on NCEP reanalysis data and ECMWF YOTC analysis data, focuses on two objectives related to the unique features of Morakot that contributed to the record-breaking rainfall. The first is to examine the translation speed change of Morakot before, during, and after TC landfall. The other is to study the southwesterly flow associated with Morakot after its landfall.

[34] Morakot's landfall on Taiwan occurred concurrently with the cyclonic phase of the intraseasonal oscillation, which enhanced the background southwesterly monsoonal flow. The extreme rainfall was caused by the very slow movement of Typhoon Morakot both in the landfall and in the postlandfall periods and the continuous formation of mesoscale convection with the moisture supply from the southwesterly flow. It is found that the amount of rainfall in Taiwan was nearly proportional to the reciprocal of TC translation speed, rather than the TC intensity.

[35] Compared with the other 18 typhoons with similar tracks, Morakot moved like a normal westward-tracking typhoon 24 h before landfall. However, its translation speed started to reduce significantly thereafter and eventually became an outlier among all the 19 typhoons. On average, these 19 typhoons showed a trend of reduced translation speed before and during landfall, but the slow-down speed of Morakot was the most dramatic. The steering flow computed from YOTC and NCEP reanalysis data agreed well with the observed translation from the JTWC best track data. When the TC center was located east of Taiwan, the PSH in the composite extended westward from southern Japan to east China and provided westward steering for the TCs. In the Morakot case, however, the TC was surrounded by low-pressure systems (associated with Typhoons Goni and Etau) and the PSH extended toward the northwest. Therefore, the strong steering effect that normally causes a TC to move westward did not exist. Instead, the steering flow was weak, resulting in the slow movement of Morakot before and during landfall. Specifically, the primary change that caused the significant speed drop of steering flow occurred at upper levels (e.g., 400 and 300 hPa) where the high-level TC circulation changed from an asymmetric to a symmetric structure. The weakening PSH, an approaching short-wave trough, and the northwestward-tilting Etau at upper levels were responsible for this transition. Furthermore, at low levels the three TC centers rotated connectedly in a counterclockwise direction along a straight axis, similar to the Fujiwhara effect, during the period of weak steering. This caused Morakot to move very slowly after landfall because it was nearly located in the center of the axis.

[36] After TC landfall, the TC circulation of Goni merged with the southwesterly flow, resulting in a southwest-northeast-oriented band of strong moisture-laden southwesterly flow extended from the eastern Bay of Bengal toward southwestern Taiwan. This moisture conveyor belt

played an important role in the heavy rainfall over southern Taiwan because it transported moist and unstable air to the southern TS and the northern SCS; herein, it converged with the typhoon circulation. Consequently, an east-west-oriented moisture band extended from southern China toward southern Taiwan. TC circulation from the northwest and the southwesterly flow were responsible for moisture transportation that led to the formation of the moisture band. This resulted in large low-level moisture flux convergence in the southern TS that moved toward southern Taiwan. Significant mesoscale convection which lasted for approximately 33 h occurred on this wind convergence line and on the mountain slopes in southern Taiwan. It is thus suggested that the long duration of Typhoon Morakot in the Taiwan area, the interaction of southwest monsoon and typhoon circulation, the mesoscale convection, and the presence of terrain, are the key factors to the tremendous rainfall.

[37] Slow translation speed and strong southwesterly flow are certainly not the only two factors that contributed to the heavy rainfall of the Morakot event. This paper is the first in a series of research studies to be conducted. Many future studies should be performed in order to fully understand this top rain producer in Taiwan's recent history. For example, the role that Goni and Etau play in the slow translation speed of Morakot can be further investigated through modeling studies. In addition, the role of Goni in enhancing the southwesterly flow and helping the moisture supply can also be numerically examined. The detail structure and evolution of the MCSs along the convective line over the southwest of Taiwan needs to be further explored. Last, the role of diabatic heating produced by the strong convection to the south of the TC in making Morakot even slower during the postlandfall period needs to be investigated.

[38] **Acknowledgments.** This research was supported by the National Science Council of Taiwan (grants NSC 97-2111-M-003-002-MY2, NSC 98-2625-M-003-001, NSC 99-2111-M-003-003, 98-2111-M-002-007-MY2, 98-2745-M-002-008-MY3, and 99-2628-M-002-MY4). We thank the Central Weather Bureau for providing numerical and observational data. We are especially grateful to C.-P. Chang, Paul Ciesielski, and Yi-Ting Yang for helpful discussions and Shih-Hao Su and Chia-Rong Chen for preparing Figures 1 and 3–5. Our gratitude also goes to the Academic Paper Editing Clinic, NTNU.

References

Carr, L. E., III, and R. L. Elsberry (1990), Observational evidence for predictions of tropical cyclone propagation relative to environmental steering, *J. Atmos. Sci.*, *47*, 542–546, doi:10.1175/1520-0469(1990)047<0542:OEFPOT>2.0.CO;2.

Carr, L. E., III, and R. L. Elsberry (1995), Monsoonal interactions leading to sudden tropical cyclone track changes, *Mon. Weather Rev.*, *123*, 265–290, doi:10.1175/1520-0493(1995)123<0265:MILTST>2.0.CO;2.

Carr, L. E., III, and R. L. Elsberry (2000), Dynamical tropical cyclone track forecast errors. Part II: Midlatitude circulation influences, *Weather Forecast.*, *15*, 662–681, doi:10.1175/1520-0434(2000)015<0662:DTCTFE>2.0.CO;2.

Chan, J. C. L., and W. M. Gray (1982), Tropical cyclone movement and surrounding flow relationship, *Mon. Weather Rev.*, *110*, 1354–1376, doi:10.1175/1520-0493(1982)110<1354:TCMASF>2.0.CO;2.

Chan, J. C. L., and R. T. Williams (1987), Analytical and numerical studies of the beta-effect in tropical cyclone motion. Part I: Zero mean flow, *J. Atmos. Sci.*, *44*, 1257–1265, doi:10.1175/1520-0469(1987)044<1257:AANSOT>2.0.CO;2.

Chang, C.-P., T.-C. Yeh, and J. M. Chen (1993), Effects of terrain on the surface structure of typhoons over Taiwan, *Mon. Weather Rev.*, *121*, 734–752, doi:10.1175/1520-0493(1993)121<0734:EOTOTS>2.0.CO;2.

Chen, G. T.-J. (1992), Mesoscale features observed in the Taiwan Mei-yu season, *J. Meteorol. Soc. Jpn.*, *70*, 497–516.

Chen, S.-J., Y.-H. Kuo, W. Wang, Z.-Y. Tao, and B. Cui (1998), A modeling case study of heavy rainstorms along the Mei-yu front, *Mon. Weather Rev.*, *126*, 2330–2351, doi:10.1175/1520-0493(1998)126<2330:AMCSOH>2.0.CO;2.

Chiao, S., and Y.-L. Lin (2003), Numerical modeling of an orographically enhanced precipitation event associated with the Tropical Storm Rachel over Taiwan, *Weather Forecast.*, *18*, 325–344, doi:10.1175/1520-0434(2003)018<0325:NMOAOE>2.0.CO;2.

Chien, F.-C., Y.-C. Liu, and C.-S. Lee (2008), Heavy rainfall and southwesterly flow after the leaving of Typhoon Mindulle (2004) from Taiwan, *J. Meteorol. Soc. Jpn.*, *86*, 17–41, doi:10.2151/jmsj.86.17.

Fiorino, M., and R. L. Elsberry (1989), Some aspects of vortex structure related to tropical cyclone motion, *J. Atmos. Sci.*, *46*, 975–990, doi:10.1175/1520-0469(1989)046<0975:SAOVSR>2.0.CO;2.

Ge, X., T. Li, Y. Wang, and M. Peng (2008), Tropical cyclone energy dispersion in a three-dimensional primitive equation model: Upper tropospheric influence, *J. Atmos. Sci.*, *65*, 2272–2289, doi:10.1175/2007JAS2431.1.

Ge, X., T. Li, S. Zhang, and M. Peng (2010), What causes the extremely heavy rainfall in Taiwan during Typhoon Morakot (2009)?, *Atmos. Sci. Lett.*, *11*, 46–50.

Holland, G. J. (1984), Tropical cyclone motion: A comparison of theory and observation, *J. Atmos. Sci.*, *41*, 68–75, doi:10.1175/1520-0469(1984)041<0068:TCMACO>2.0.CO;2.

Hong, C.-C., M.-Y. Lee, H.-H. Hsu, and J.-L. Kuo (2010), Role of submonthly disturbance and 40–50 day ISO on the extreme rainfall event associated with Typhoon Morakot (2009) in southern Taiwan, *Geophys. Res. Lett.*, *37*, L08805, doi:10.1029/2010GL042761.

Jian, G.-J., and C.-C. Wu (2008), A numerical study of the track deflection of super-Typhoon Haitang (2005) prior to its landfall in Taiwan, *Mon. Weather Rev.*, *136*, 598–615, doi:10.1175/2007MWR2134.1.

Kalnay, E., et al. (1996), The NCEP/NCAR 40-Year Reanalysis Project, *Bull. Am. Meteorol. Soc.*, *77*, 437–471, doi:10.1175/1520-0477(1996)077<0437:TNYRP>2.0.CO;2.

Kanamitsu, M., W. Ebisuzaki, J. Woollen, S.-K. Yang, J. J. Hnilo, M. Fiorino, and G. L. Potter (2002), NCEP-DOE AMIP-II Reanalysis (R-2), *Bull. Am. Meteorol. Soc.*, *83*, 1631–1643, doi:10.1175/BAMS-83-11-1631(2002)083<1631:NAR>2.3.CO;2.

Lee, C.-S., Y.-C. Liu, and F.-C. Chien (2008), The secondary low and heavy rainfall associated with Typhoon Mindulle (2004), *Mon. Weather Rev.*, *136*, 1260–1283, doi:10.1175/2007MWR2069.1.

Lin, Y.-L., J. Han, D. W. Hamilton, and C.-Y. Huang (1999), Orographic influence on a drifting cyclone, *J. Atmos. Sci.*, *56*, 534–562, doi:10.1175/1520-0469(1999)056<0534:OIOADC>2.0.CO;2.

Lin, Y.-L., D. B. Ensley, S. Chiao, and C.-Y. Huang (2002), Orographic influences on rainfall and track deflection associated with the passage of a tropical cyclone, *Mon. Weather Rev.*, *130*, 2929–2950, doi:10.1175/1520-0493(2002)130<2929:OIORAT>2.0.CO;2.

Liu, K. S., and J. C. L. Chan (2008), Interdecadal variability of western North Pacific tropical cyclone tracks, *J. Clim.*, *21*, 4464–4476, doi:10.1175/2008JCLI2207.1.

Trier, S. B., D. B. Parsons, and T. J. Matejka (1990), Observations of a subtropical cold front in a region of complex terrain, *Mon. Weather Rev.*, *118*, 2449–2470, doi:10.1175/1520-0493(1990)118<2449:OOASCF>2.0.CO;2.

Wu, C.-C. (2001), Numerical simulation of Typhoon Gladys (1994) and its interaction with Taiwan terrain using GFDL hurricane model, *Mon. Weather Rev.*, *129*, 1533–1549, doi:10.1175/1520-0493(2001)129<1533:NSOTGA>2.0.CO;2.

Wu, C.-C., and K. A. Emanuel (1995a), Potential vorticity diagnostics of hurricane movement. Part I: A case study of Hurricane Bob (1991), *Mon. Weather Rev.*, *123*, 69–92, doi:10.1175/1520-0493(1995)123<0069:PVDOHM>2.0.CO;2.

Wu, C.-C., and K. A. Emanuel (1995b), Potential vorticity diagnostics of hurricane movement. Part II: Tropical Storm Ana (1991) and Hurricane Andrew (1992), *Mon. Weather Rev.*, *123*, 93–109, doi:10.1175/1520-0493(1995)123<0093:PVDOHM>2.0.CO;2.

Wu, C.-C., and Y.-H. Kuo (1999), Typhoons affecting Taiwan: Current understanding and future challenges, *Bull. Am. Meteorol. Soc.*, *80*, 67–80, doi:10.1175/1520-0477(1999)080<0067:TATCUA>2.0.CO;2.

Wu, C.-C., T.-H. Yen, Y.-H. Kuo, and W. Wang (2002), Rainfall simulation associated with Typhoon Herb (1996) near Taiwan. Part I: The topographic effect, *Weather Forecast.*, *17*, 1001–1015, doi:10.1175/1520-0434(2003)017<1001:RSAWTH>2.0.CO;2.

Wu, C.-C., T.-S. Huang, and K.-H. Chou (2004), Potential vorticity diagnosis of the key factors affecting the motion of Typhoon Sinlaku (2002), *Mon. Weather Rev.*, *132*, 2084–2093, doi:10.1175/1520-0493(2004)132<2084:PVDOTK>2.0.CO;2.

Wu, C.-C., K. K. W. Cheung, and Y.-Y. Lo (2009), Numerical study of the rainfall event due to the interaction of Typhoon Babs (1998) and the northeasterly monsoon, *Mon. Weather Rev.*, *137*, 2049–2064, doi:10.1175/2009MWR2757.1.

Yeh, T.-C., and R. L. Elsberry (1993a), Interaction of typhoons with the Taiwan orography. Part I: Upstream track deflections, *Mon. Weather Rev.*, *121*, 3193–3212, doi:10.1175/1520-0493(1993)121<3193:IOTWTT>2.0.CO;2.

Yeh, T.-C., and R. L. Elsberry (1993b), Interaction of typhoons with the Taiwan orography. Part II: Continuous and discontinuous tracks across the island, *Mon. Weather Rev.*, *121*, 3213–3233, doi:10.1175/1520-0493(1993)121<3213:IOTWTT>2.0.CO;2.

F.-C. Chien, Department of Earth Sciences, National Taiwan Normal University, No. 88, Sect. 4, Ting-Chou Road, Taipei 11677, Taiwan. (jfj@ntnu.edu.tw)

H.-C. Kuo, Department of Atmospheric Sciences, National Taiwan University, Taipei 10617, Taiwan.